DEDD regulates degradation of intermediate filaments during apoptosis

Justine C. Lee,[1] Olaf Schickling,[1] Alexander H. Stegh,[1] Robert G. Oshima,[2] David Dinsdale,[3] Gerald M. Cohen,[3] and Marcus E. Peter[1]

[1]The Ben May Institute for Cancer Research, University of Chicago, Chicago, IL 60637
[2]The Burnham Institute, La Jolla, CA 92037
[3]Medical Research Council Toxicology Unit, University of Leicester, Leicester LE1 9HN, United Kingdom

Apoptosis depends critically on regulated cytoskeletal reorganization events in a cell. We demonstrate that death effector domain containing DNA binding protein (DEDD), a highly conserved and ubiquitous death effector domain containing protein, exists predominantly as mono- or diubiquitinated, and that diubiquitinated DEDD interacts with both the K8/18 intermediate filament network and pro–caspase-3. Early in apoptosis, both cytosolic DEDD and its close homologue DEDD2 formed filaments that colocalized with and depended on K8/18 and active caspase-3. Subsequently, these filamentous structures collapsed into intracellular inclusions that migrated into cytoplasmic blebs and contained DEDD, DEDD2, active caspase-3, and caspase-3–cleaved K18 late in apoptosis. Biochemical studies further confirmed that DEDD coimmunoprecipitated with both K18 and pro–caspase-3, and kinetic analyses placed apoptotic DEDD staining prior to caspase-3 activation and K18 cleavage. In addition, both caspase-3 activation and K18 cleavage was inhibited by expression of DEDDΔNLS1-3, a cytosolic form of DEDD that cannot be ubiquitinated. Finally, siRNA mediated DEDD knockdown cells exhibited inhibition of staurosporine-induced DNA degradation. Our data suggest that DEDD represents a novel scaffold protein that directs the effector caspase-3 to certain substrates facilitating their ordered degradation during apoptosis.

Introduction

Apoptosis is a fundamental cell elimination process central to homeostasis regulation in all tissues. Dysregulation of apoptosis can result in many pathological processes such as degenerative diseases and cancer (Peter et al., 1997). Cells undergoing apoptosis show a sequence of cardinal morphological features including membrane blebbing, cellular shrinkage, and condensation and fragmentation of the nuclei (Wyllie et al., 1980; Earnshaw, 1995), most of which depend on activation of caspases (Earnshaw et al., 1999; Stegh and Peter, 2001). In epithelial cells, caspase-3, -6, and -7 are involved in the cleavage of intermediate filament (IF)* proteins such as cytokeratins, which is an important step during the disintegration of cells (Caulin et al., 1997; Ku et al., 1997, 2002). However, little is known about the mechanisms that ensure the ordered disintegration of cytoplasmic caspase substrates.

We recently identified a protein that we called death effector domain containing DNA binding protein (DEDD). Among apoptosis signaling molecules, DEDD is unique, both in its abundance and its conservation between species, indicating an essential involvement in an evolutionarily universal process (Stegh et al., 1998). DEDD contains three nuclear localization signals and binds DNA and chromatin with high affinity but predominantly resides in the cytoplasm, suggesting that DEDD functions as a communicator between the cytoplasm and nucleus (Stegh et al., 1998; Schickling et al., 2001). Similar to several other DED proteins, overexpression experiments suggested that DEDD was a proapoptotic molecule. In contrast to all other DED proteins, DEDD requires nuclear localization to induce apoptosis, suggesting that it engages a novel nuclear apoptosis pathway (Schickling et al., 2001). In the nucleoli, it activates and colocalizes with active caspase-6 and interacts with a novel DED binding protein DEDAF (Zheng et al., 2001).

We now show that in many cells cytosolic DEDD is expressed mostly in a diubiquitinated form which associates

The online version of this article contains supplemental material.

Address correspondence to Marcus Peter, The Ben May Institute for Cancer Research, University of Chicago, 924 E. 57th Street, Chicago, IL 60637. Tel.: (773) 702-4728. Fax: (773) 702-3701. E-mail: MPeter@ben-may.bsd.uchicago.edu

J.C. Lee and O. Schickling contributed equally to this work.

*Abbreviations used in this paper: DEDD, death effector domain containing DNA binding protein; IF, intermediate filament; STS, staurosporine.

Key words: apoptosis; caspases; DEDD; intermediate filaments; mono-ubiquitination

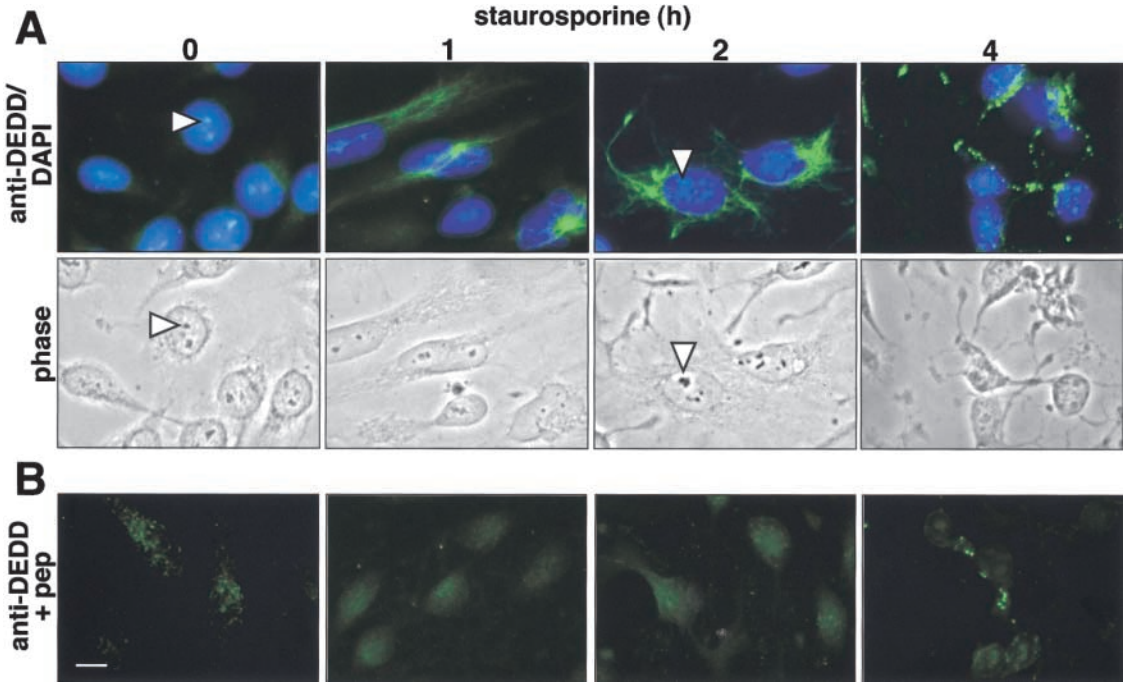

Figure 1. **DEDD aggregates and forms filaments in apoptotic cells.** (A) HeLa cells treated with 1 μM STS for 0, 1, 2, or 4 h and stained with an anti-DEDD antibody (DED3) demonstrates both a dramatic differential subcellular localization of DEDD and an increase in the intensity of DEDD staining after the initiation of apoptosis. The low level of cytoplasmic staining detected in unstimulated cells was also found with control rabbit IgG (not depicted). Nuclei were visualized using DAPI (2 μg/ml). Arrowheads denote nucleoli. (B) HeLa cells were treated as in (A) and stained with DED3 in the presence of the DED3-peptide (pep) leading to a competition for the binding sites of the antibody. Bar, 10 μm.

with both keratin 18 and procaspase-3. Upon induction of apoptosis, cytosolic DEDD first aggregates and then stains in filamentous structures associated with the cytokeratin 8/18 network in a strictly caspase-3–dependent fashion. We also report the cloning of a close homologue of DEDD, which was recently reported as DEDD2 (Roth et al., 2002) or FLAME3 (Zhan et al., 2002). Using an antibody against the DED of DEDD2, we demonstrate that DEDD2 can also be stained on IFs in apoptosing cells. As apoptosis progresses, K18 is cleaved by caspase-3 and reorganizes into intracellular inclusions that colocalize with DEDD, DEDD2, and active caspase-3. Expression of a cytosolic dominant negative version of DEDD inhibits activation of caspase-3 and the subsequent cleavage of K18. Therefore, we conclude that DEDD is important for the degradation of the IF system by caspase-3 and execution of apoptosis in epithelial cells.

Results

DEDD forms filamentous aggregates in apoptosing cells

During immunofluorescence microscopy of untreated HeLa cells, DEDD was detected using the DED3 antibody in nucleoli (Fig. 1 A) but virtually undetectable in the cytoplasm. However, 1 h after induction of apoptosis with staurosporine (STS), DEDD stained as filamentous aggregates that seemed to originate from a perinuclear structure. After 2 h, these filamentous structures expanded to fill the entire cytosol of apoptotic cells. In the final stage of apoptosis, coinciding with nuclear fragmentation, these DEDD filaments disintegrated into bright inclusions (4 h of STS treatment). Specificity of DEDD staining was confirmed by competition with the DED3 peptide (Fig. 1 B). These data suggested that the DED3-specific epitope in the native conformation of DEDD becomes available in cells undergoing apoptosis. During the course of apoptosis, nucleolar DEDD staining was progressively reduced until undetectable at late stages. This phenomenon appeared to be independent of nucleolar segregation, as evidenced by the persistence of nucleolar structures in phase contrast even after the loss of nucleolar DEDD staining (2 h postinduction, Fig. 1 A, arrowhead). These data suggested that during apoptosis, nucleolar DEDD either leaves nucleoli or changes its conformation so that it cannot be detected by DED3. It is unlikely that DEDD is degraded by caspases because we have not found it to be a caspase substrate at these time points (unpublished data). We conclude that cytosolic DEDD either associates with or forms cytoplasmic filaments in an apoptosis dependent manner.

Formation of filamentous DEDD structures requires caspase-3

Apoptosis induction was required to detect DEDD in filamentous structures. This prompted us to test whether caspases regulated DEDD filament formation. We first treated HeLa cells with STS for 2 h in the absence and presence of the poly-caspase inhibitor zVAD-fmk and found significant inhibition of cytosolic DEDD filaments by zVAD-fmk (unpublished data). These data suggested that caspases played a role in regulating the formation of DEDD aggregates. To determine the contribution of the main effector caspase-3 to this process, we tested MCF7 cells which do not express caspase-3 (Janicke et al., 1998b) and compared them to cells re-

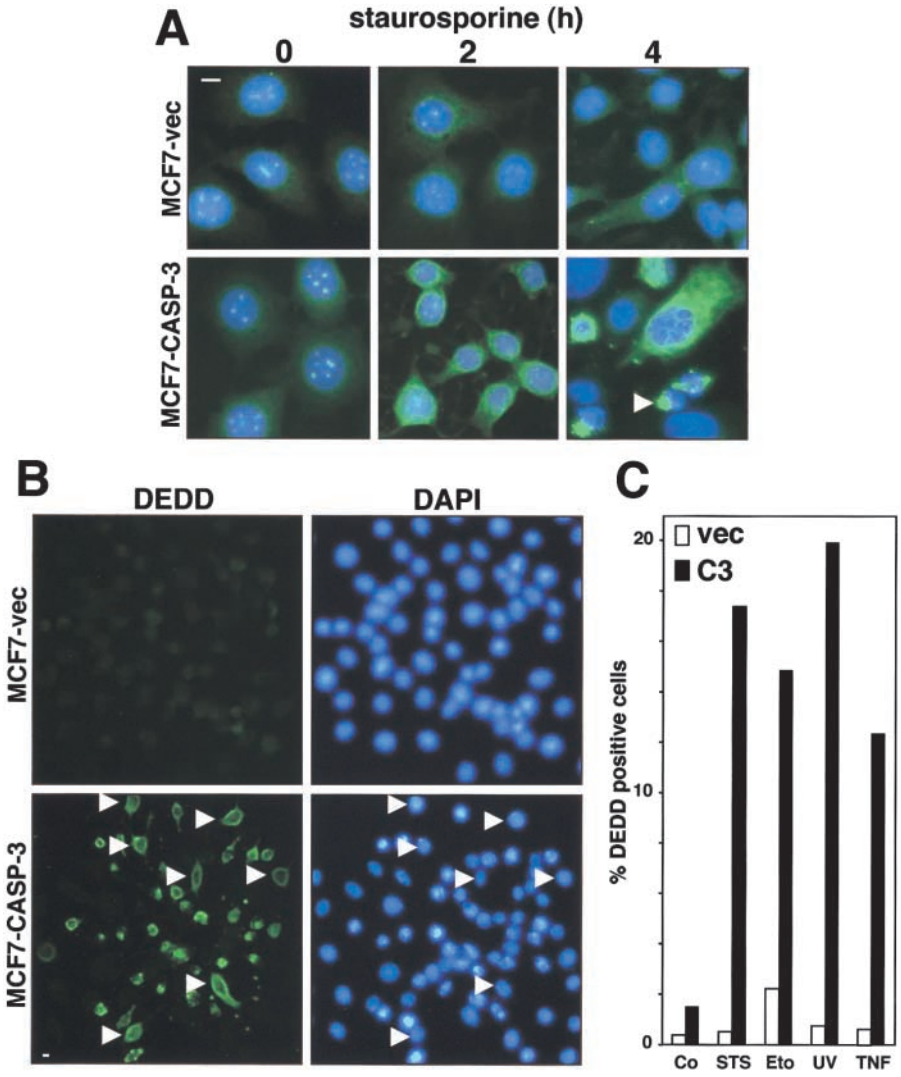

Figure 2. **Filamentous DEDD requires caspase-3 and precedes nuclear changes in apoptosis.** (A) MCF7-vec and MCF7-C3 cells were treated with 1 μM STS for 0, 2, and 4 h and stained with DED3. Arrowhead denotes a strong DEDD-positive structure in a cell at a late stage of apoptosis. (B) MCF7-vec and MCF7-C3 cells were incubated for 4 h with 1 μM STS and stained with DED3. Arrowheads in the MCF7-C3 panels indicate cells that contain large amounts of DEDD filaments but lack apoptotic nuclear changes. Bar, 10 μm. (C) Apoptosis-induced increase in DEDD staining was quantified via an intracellular FACS-based analysis in MCF7-vec (vec) and MCF7-C3 (C3) cells treated with a variety of apoptotic stimuli. Co, untreated control; Eto, etoposide; STS, staurosporine; TNF, tumor necrosis factor α; UV, UV irradiation.

constituted with procaspase-3 (MCF7-C3). In both MCF7-vec and MCF7-C3 cells, DEDD was only detectable in nucleoli prior to induction of apoptosis (Fig. 2 A). After treatment of MCF7-vec cells with STS for 2 h, DEDD continued to be detected exclusively in nucleoli, which started to segregate. 4 h after treatment most DEDD reactivity had diminished (Fig. 2 A). The cells eventually detached and underwent apoptosis (as judged by nuclear condensation; unpublished data) without the detection of DEDD filaments. In contrast, MCF7-C3 cells displayed both a change in DEDD compartmentalization as well as highly ordered structures during apoptosis. After 2 h of STS treatment, DEDD filaments were detected surrounding the nucleus. After 4 h of STS treatment massive amounts of DEDD filaments formed in these cells (Fig. 2 A). At later stages, the filaments appeared to fall apart leaving behind brightly stained DEDD-positive inclusions (Fig. 2 A, arrowhead). These experiments demonstrated that detection of DEDD in filamentous structures requires active caspase-3. Fig. 2 B supports this strict dependence on caspase-3. The majority of the MCF7-C3 but none of the MCF7-vec cells became positive when stained with the DED3 antibody. This experiment also demonstrated that cells containing elongated DEDD filaments showed no signs of nuclear changes such as condensation and nuclear fragmentation (Fig. 2 B, arrowheads). However, all cells with disintegrated DEDD filaments and DEDD-positive inclusions exhibited such nuclear changes, suggesting that formation of DEDD filaments precedes nuclear disintegration. During apoptosis, DEDD undergoes a caspase-3–dependent change which exposes the epitope in the DED recognized by DED3.

To determine the generality of DEDD filament formation, we quantified the increase of caspase-3–dependent DEDD staining using different forms of apoptosis induction and established a FACS-based assay in permeabilized cells (Fig. 2 C). All apoptosis stimuli tested (STS, etoposide, UV, and TNFα) resulted in a clear increase in intracellular DEDD staining, again only in the MCF7 cells reconstituted with procaspase-3. In all cases we also detected DEDD in filamentous structures (unpublished data). Thus, this behavior of DEDD is a general phenomenon that can be observed whenever caspase-3 is activated.

DEDD is a mono- and diubiquitinated protein

Two different anti-DEDD antibodies, PRO29 and DED3, detected three protein forms of DEDD at 54, 44, and the

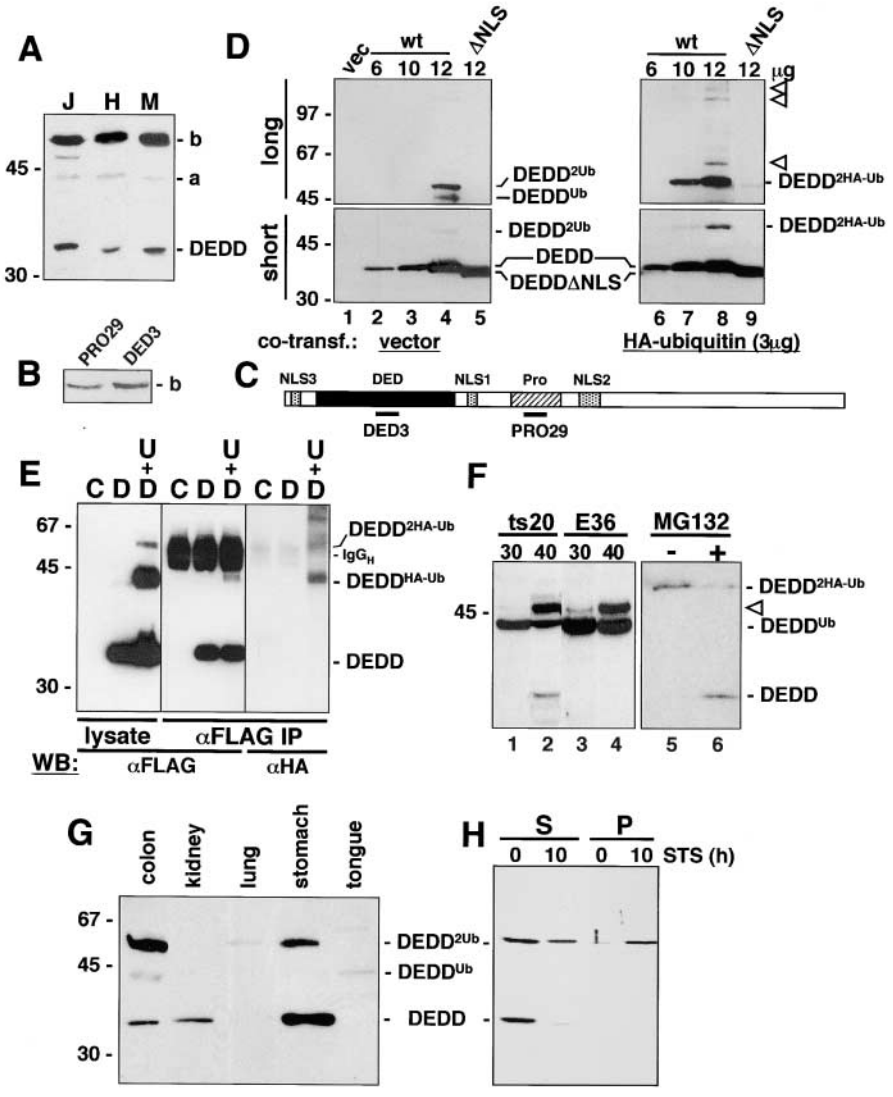

Figure 3. **DEDD is mono- and diubiquitinated.** (A) Western blot analysis of endogenous DEDD detected with the PRO29 antibody in total cellular lysates of Jurkat (J), HeLa (H), and MCF7 (M) cells. a and b represent higher forms of DEDD at 44 and 54 kD, respectively. (B) Both anti-DEDD antibodies, PRO29 and DED3, detect band b in Western blots of the total cellular extracts of HeLa cells. (C) Schematic representation of the DEDD molecule. Sites of peptides used for the generation of the two rabbit polyclonal anti-DEDD antibodies DED3 and PRO29 are indicated. (D) 293T cells were transfected with 12 μg pcDNA3 (vec), DEDD-FLAG (wt), or DEDDΔNLS (ΔNLS) at the indicated amounts, in the absence (lanes 1–5) or presence (lanes 6–9) of HA-ubiquitin and Western blotted with anti-FLAG. Short (bottom) and long (top) exposures are shown. Reprobe of blots with anti-HA yielded dark lanes in those cotransfected with HA-ubiquitin (not depicted). Arrowheads denote a higher species of DEDD after HA-ubiquitin cotransfection. (E) 293T cells were transfected with vector (C), DEDD-FLAG (D), or DEDD-FLAG plus HA-ubiquitin (D + U). DEDD was immunoprecipitated with anti-FLAG (middle and right) and lysates (left) and precipitates were analyzed by Western blotting with either anti-FLAG (left and middle) or anti-HA (right). To better separate ubiquitinated DEDD from the IgG heavy chain (IgG_H), conditions were chosen that resulted predominantly in formation of monoubiquitinated DEDD. (F) Temperature sensitive E1 mutant (ts20) and parental (E36) cell lines were cultured at the permissive temperature (30°C, lanes 1 and 3) and restrictive temperature (40°C, lanes 2 and 4) for 12 h and blotted with PRO29. Arrowhead denotes an unknown band found in both cell lines at the restrictive temperature. Additionally, deubiquitination of DEDD was also observed in 293T cells transfected with HA-ubiquitin and mock treated (lane 5) or treated with 20 μM MG132 for 12 h (lane 6). (G) Proteins extracted from murine tissues were blotted with PRO29. Note that the blot shown represents one of four independent mice (two male, two female) bearing similar results. (H) Jurkat cells were treated with 1 μM STS for 10 h, lysed and separated into a detergent soluble (S) and an insoluble (P) fraction. DEDD was visualized by Western blotting using PRO29. $DEDD^{Ub}$, monoubiquitinated DEDD; $DEDD^{2Ub}$, diubiquitinated DEDD; $DEDD^{2HA\text{-}Ub}$, HA-tagged diubiquitinated DEDD. All M_r notations on left side of blots in kD.

expected 37 kD (Fig. 3, A and B; unpublished data). These three bands were spaced by ~8 kD, suggesting a covalent modification of 8 kD, the size of ubiquitin. Therefore, we tested whether the higher DEDD bands corresponded to mono and diubiquitinated DEDD. This analysis was complicated by the fact that the higher forms of DEDD cannot be directly immunoprecipitated from cellular lysates due to their insolubility (unpublished data). To test whether higher DEDD bands could be detected upon overexpression of DEDD, we transiently transfected 3′FLAG-tagged DEDD (DEDD-FLAG) into 293T cells. Transfection of DEDD-FLAG resulted in a weakly reactive 55-kD band (Fig. 3 D, lane 4, bottom). Upon longer exposure of the same immunoblot, a faster migrating band at 45 kD was also detected (Fig. 3 D, lane 4, top). These two FLAG reactive bands likely represented the FLAG-tagged versions of the endogenous 54- and 44-kD bands. Cotransfection of the same amounts of DEDD-FLAG in the presence of HA-tagged ubiquitin (Fig. 3 D, lanes 6–8) resulted in a much more efficient formation of FLAG-reactive bands migrating above DEDD-FLAG (Fig. 3 D, lane 8). The detected band migrated ~4 kD slower than the highest band in cells transfected with DEDD-FLAG, consistent with DEDD-FLAG modified by two HA-ubiquitin (10 kD) rather than two endogenous ubiquitin (8 kD) peptides. These data strongly suggested that DEDD was a diubiquitinated protein. We also detected higher molecular weight forms of DEDD likely corresponding to higher order ubiquitinated DEDD (Fig. 3 D, lane 8, top, arrowheads). To confirm the formation of monoubiquitinated DEDD in 293T cells, we cotransfected cells with DEDD-FLAG and HA-ubiquitin and immunoprecipitated DEDD with anti-FLAG (Fig. 3

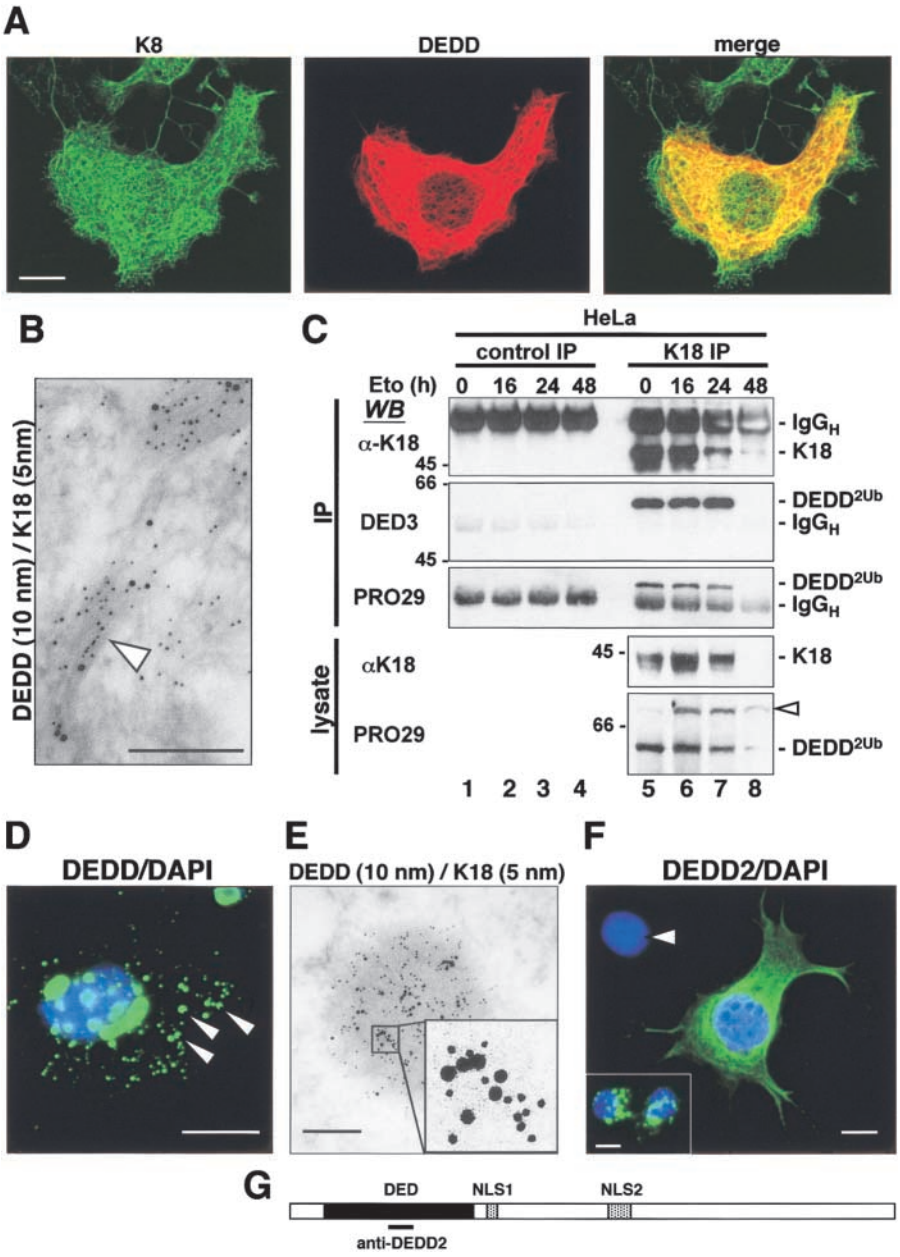

Figure 4. **DEDD associates with K18.** (A) Apoptosis was induced in MCF7-C3 cells (4 h, 1 μM STS) and stained with DED3 and anti-K8 for confocal microscopy. Shown are two-dimensional pictures of three-dimensional images, which were created using 20 overlaying 0.5 μm z-sections. Merge panel is an overlay of the K8 and DEDD staining. Very significant colocalization was also seen on individual sections (not depicted). Bar, 10 μm. (B) Electron microscopy of HeLa cells treated with TRAIL (2 h) detected DEDD and K18 in filamentous structures using immunogold labeling. Arrowhead denotes a characteristic K18 10-nm filament. Note that these filaments appear shorter than usual likely due to the onset of apoptosis. Bar, 200 nm. (C) Solubilization and immunoprecipitation of K18 in non-apoptosing and apoptosing (treated with etoposide [Eto] for 16, 24, or 48 h) HeLa cells coimmunoprecipitated DEDD as detected by both DED3 and PRO29 antibodies. 1C4, an anti-FADD antibody, was used as an IgG1 control immunoprecipitation. IgG_H, IgG heavy chain. Arrowhead denotes higher DEDD reactive band formed upon Eto treatment. All M_r notations on left side of blots in kD. (D) MCF7-C3 cells were treated with STS (1 μM) for 8 h, fixed with paraformaldehyde, stained with DED3 and DAPI, and visualized by fluorescence microscopy. Arrowheads indicate DEDD-containing intracellular inclusions found in late stages of apoptosis after filament disintegration and coinciding with nuclear changes. Bar, 10 μm. (E) A549 cells were treated with TRAIL (1 μg/ml, 3 h) and subjected to immunoelectron microscopy. A typical intracellular inclusion found late in apoptosis is shown labeled by both DED3 (labeled with 10-nm gold particles) and anti-K18 (labeled with 5-nm gold particles). Bar, 200 nm. (F) DEDD filaments and intracellular inclusions (inset) in MCF7-C3 cells stained with anti-DEDD2 after apoptosis induction (1 μM STS, 4 h). Bar, 10 μm. Arrowhead, nucleus of nonapoptosing cell, which did not stain with anti-DEDD2. (G) Schematic representation of DEDD2. Site of the peptide used for the generation of the rabbit polyclonal anti-DEDD2 antibody is indicated.

E). A positive signal with anti-HA in Western blotting confirmed the identity of the 46-kD band as monoubiquitinated DEDD (Fig. 3 E, right).

Conversely, to test whether endogenous DEDD was mono- and/or diubiquitinated, we analyzed DEDD in a system that lacked ubiquitination capabilities such as the hamster cell line ts20 that expresses a temperature-sensitive mutant of the ubiquitin-activating E1 enzyme (Zhande et al., 2002). Because human DEDD is virtually identical to mouse and rat DEDD, we expected our antibodies to detect hamster DEDD. At the permissive temperature (30°C), Western blot analysis revealed that these cells mainly express the 44-kD DEDD species (Fig. 3 F, lane 1). However, after inactivation of E1 at the restrictive temperature (40°C), a significant amount of the 44-kD band disappeared which paralleled with the appearance of 37 kD unmodified DEDD (Fig. 3 F, lane 2). This effect was not seen in the control cell line E36 (Fig. 3 F, lane 4), suggesting that the monoubiquitinated DEDD was deubiquitinated in the absence of functional E1. These data indicate that DEDD is mono- and diubiquitinated. Interestingly, a recently described DEDD mutant lacking all three NLS could not be significantly ubiquitinated (Fig. 3 D, lane 9). This could be due to either the deletion of the ubiquitinated lysine residue(s) that could be part of the NLS or to the mutation of critical residues that facilitate binding of the ubiquitinating enzymes.

Unlike polyubiquitination, the role of monoubiquitination does not appear to be to target proteins to the protea-

some-mediated degradative pathway. In fact, treatment of cells with proteasome inhibitors has been reported to result in deubiquitination of monoubiquitinated proteins such as histone H2A and H2B (Mimnaugh et al., 1997) and the HIV-1 $p6^{Gag}$ protein (Schubert et al., 2000), likely due to the depletion of cells of free ubiquitin which gets bound to accumulating polyubiquitinated proteins. To test whether diubiquitinated DEDD would also be deubiquitinated in cells treated with proteasome inhibitors we transiently transfected 293T cells with HA-ubiquitin (resulting in detection of only diubiquitinated endogenous DEDD) and treated with 20 μM of MG132 for 12 h (Fig. 3 F, lane 6). A complete conversion of 55 kD DEDD into 37 kD DEDD was detected, consistent with DEDD being deubiquitinated. To confirm the existence of both the mono- and the diubiquitinated DEDD species in primary cells, we tested expression of DEDD in tissues of mice (Fig. 3 G). Kidney expresses mainly unmodified DEDD, and tongue and lung contain mainly mono- and diubiquitinated DEDD, respectively, and colon and lung expressed mixtures of different DEDD species. These data indicated tissue specificity in DEDD expression and ubiquitination.

We noticed that ubiquitinated DEDD is less soluble than unmodified DEDD (unpublished data) consistent with our observation that DEDD-FLAG was more efficiently immunoprecipitated than HA-Ubi-DEDD-FLAG (Fig. 3 E). Induction of apoptosis in Jurkat T cells by STS coincided with a disappearance of the 37-kD DEDD band in the detergent soluble fraction and an appearance of diubiquitinated DEDD in the detergent insoluble fraction (Fig. 3 H). This change in solubility was recapitulated in fractionation of HeLa cells (unpublished data). Further characterization of these fractions identified cytoskeletal proteins, such as keratin 8 (K8), specifically fractionated as detergent insoluble corresponding to the low solubility of keratins in NP-40. Thus, the newly formed $DEDD^{2Ub}$ cofractionated with K8 in HeLa cells indicating that $DEDD^{2Ub}$ possessed solubility properties of cytoskeletal proteins.

DEDD colocalizes and associates with cytokeratin 8/18

Apoptotic DEDD-positive filamentous structures strongly resembled filamentous structures formed by cytoskeletal proteins, suggesting that DEDD may interact with the cytoskeleton. To test this, we stained cells for DEDD, actin, microtubules, and cytokeratins. We did not detect a colocalization of DEDD with either actin or microtubules (unpublished data). However, DEDD appeared to colocalize with cytokeratins in STS treated MCF7-caspase-3 cells (Fig. 4 A). We chose to stain for cytokeratin 8 (K8), as it is known that K8, compared with K18, is much more resistant to caspase cleavage (Caulin et al., 1997; Ku et al., 1997). Interestingly, confocal microscopy indicated that not all IFs stained positive for DEDD, but virtually all DEDD-positive structures were stained with the K8 antibody. A similar result was obtained when cells were costained for DEDD and K18 (unpublished data). A costaining of DEDD with K18 in IF structures was also observed in HeLa cells treated with TRAIL for 2 h using electron microscopy and immunogold labeling (Fig. 4 B). Because DEDD is only detectable in apoptosing cells by microscopy, these experiments did not address whether DEDD was constantly associated with the IF system with the DED3 epitope becoming accessible during apoptosis or whether it associated with cytokeratins in a stimulation dependent manner. To determine whether DEDD was associated with K18 in nonapoptosing cells, we performed an immunoprecipitation experiment using an anti-K18 antibody with the detergent Empigen BB, reported to solubilize ~40% of cellular cytokeratins in simple epithelial cell lines (Lowthert et al., 1995). In agreement with our cell fractionation results, DEDD coimmunoprecipitated with full length K18 (Fig. 4 C). Specifically, the coimmunoprecipitated band was $DEDD^{2Ub}$ and could again be detected with both anti-DEDD antibodies. When apoptosis was induced by treating these cells with etoposide for 48 h, K18 was completely degraded in these cells and consequently DEDD could no longer be immunoprecipitated with the anti-K18 antibody (Fig. 4 C, lane 8), suggesting that in these cells, $DEDD^{2Ub}$ stays bound to K18 throughout the apoptosis induction. Interestingly, we detected the appearance of higher forms of DEDD that could point to an apoptosis induced ubiquitination of DEDD during this treatment (Fig. 4 C, bottom, arrowhead).

Late during apoptosis, the IF networks collapse and all caspase-cleaved and disintegrated cytokeratins are found in intracellular inclusions (MacFarlane et al., 2000). Like cytokeratins, DEDD was also detected in granular structures late in apoptosis (Fig. 4 D) which could be observed in the phase contrast as dark structures (unpublished data). Therefore, we tested whether these DEDD-containing structures were identical to the keratin-containing inclusions previously described. Using different sized gold particles conjugated to secondary antibodies, we performed a costaining analysis using electron microscopy (Fig. 4 E) on TRAIL-treated A549 cells. DEDD completely colocalized with keratin 18 (Fig. 4 E) and vimentin (unpublished data) in these structures, confirming that the DEDD-positive granules detected in this work are identical to the previously described inclusion bodies. We performed this analysis using EM because it was previously shown that the inclusions are filled with tightly packed amorphous protein such that the interior of the inclusion is impenetrable by antibodies in confocal microscopy, a phenomenon also observed for DEDD (unpublished data). Interestingly, when we used an antibody against the DED of DEDD2 to stain STS-treated MCF7-C3 cells, we detected DEDD2 in both IF like filamentous structures (Fig. 4 F) and, at later stages of apoptosis, in the same inclusions as DEDD (Fig. 4 F, inset), suggesting that DEDD and DEDD2 act together.

DEDD partially colocalizes with caspase-3–cleaved K18

During apoptosis induced by various methods, many type I keratins are cleaved by caspases (Oshima, 2002) resulting in disintegration of the IF system. Two cleavage sites have been identified in K18 (Fig. 5 A). Asp238, in the center of the molecule is cleaved by both caspase-3/7 and caspase-6 and Asp397, at the COOH terminus, is specific for caspase-3/7 cleavage. Cleavage at D397 occurs early during apoptosis and generates a neoepitope reactive with the commercially available antibody M30, that can be used to monitor caspase-3 activation (Leers et al., 1999). Caspase-mediated cleavage of K18 (48.1 kD) generates 45-, 26.3-, and 19-kD

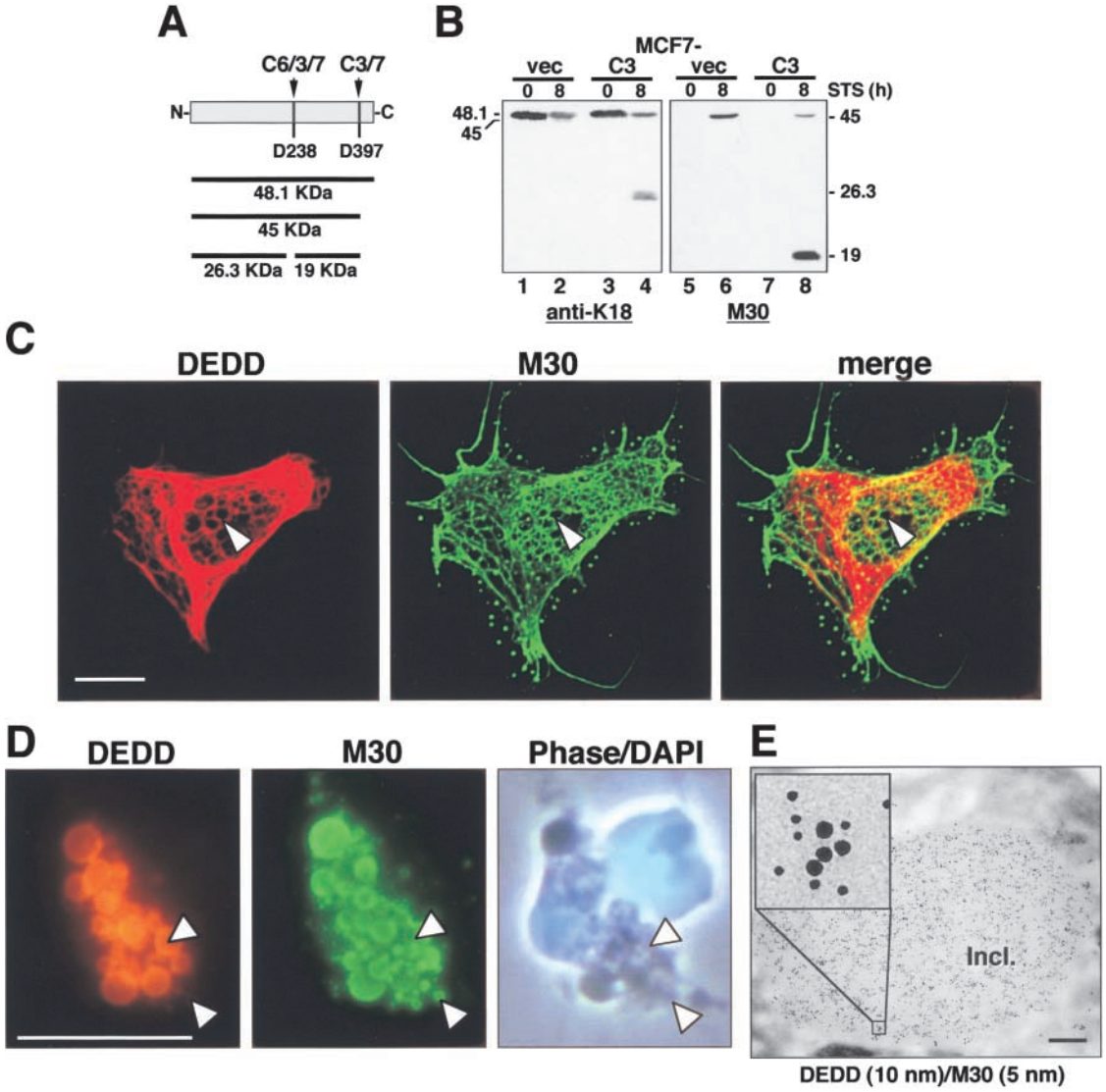

Figure 5. **Caspase-3–dependent K18 cleavage products colocalize with apoptotic DEDD structures.** (A) Scheme of the caspase-cleavage of K18. (B) Total cellular lysates of MCF7-vec and MCF7-C3 cells before and after induction of apoptosis (STS 1 μM, 8 h) were blotted with anti-K18 and M30 to detect keratin cleavage. Sizes in kD correspond to fragment sizes in A. (C) Early apoptotic MCF7-C3 cells (treated with STS 1 μM, 4 h) displayed colocalization of DEDD and cleaved K18 filaments in confocal microscopy as detected by DED3 and M30. Shown are 2D-pictures of 3D-images, which were created using 20 overlaying 0.5 μm z-sections. Merge, overlay of the M30 and DEDD staining. Bar, 10 μm. (D) Late apoptotic MCF7-C3 cells (200 μM etoposide, 24 h) displayed colocalization of DEDD and cleaved K18 in intracellular inclusions in confocal microscopy as detected by DED3 and M30. Shown are two-dimensional pictures of three-dimensional images, which were created using 20 overlaying 0.5 μm z-sections. Selected cytoplasmic blebs containing DEDD and caspase-3–cleaved K18 are labeled by arrowheads. Bar, 10 μm. (E) A549 cells treated with TRAIL (1 μg/ml) for 3 h were subjected to immunoelectron microscopy. Late apoptotic intracellular inclusions (Incl.) were found to contain both DEDD, detected by DED3 (10 nm gold particles), and cleaved K18, detected by M30 (5-nm gold particles). Bar, 400 nm.

fragments (Caulin et al., 1997; Ku et al., 1997). In both MCF7-vec and MCF7-C3 cells, STS treatment generated the 45 kD large fragment (D397 cleavage), which migrates close to the full-length K18, demonstrating that caspase-3 is not absolutely required for cleavage at D397 (Fig. 5 B, lanes 2, 4, 6, and 8). However, complete cleavage of K18 at both D238 and D397 was markedly different between MCF7-vec and MCF7-C3. STS treatment (8 h) of MCF7-C3 cells resulted in a significant amount of K18 cleavage based on the generation of the 26.3-kD fragment, identifying the epitope of the anti-K18 mAb in the NH_2-terminal half of the protein (Fig. 5 B, lane 4). Under the same conditions, the M30 Ab detected two fragments (45 and 19 kD), both of which must contain the neoepitope formed after cleavage of K18 at position D397 (Fig. 5 B, lane 8). The absence of both the 26.3- (Fig. 5 B, lane 2) and the 19-kD (Fig. 5 B, lane 6) fragments in MCF7-vec cells indicates that the K18 cleavage at D238 requires caspase-3.

Because DEDD associated with cytokeratin 8/18, we tested whether an association between caspase-3 (M30 positive)-cleaved K18 and DEDD could be established (Fig. 5 C). A confocal microscopic analysis showed that a small but significant amount of DEDD colocalized with caspase-3–cleaved K18 in the center, but not in the periphery of the

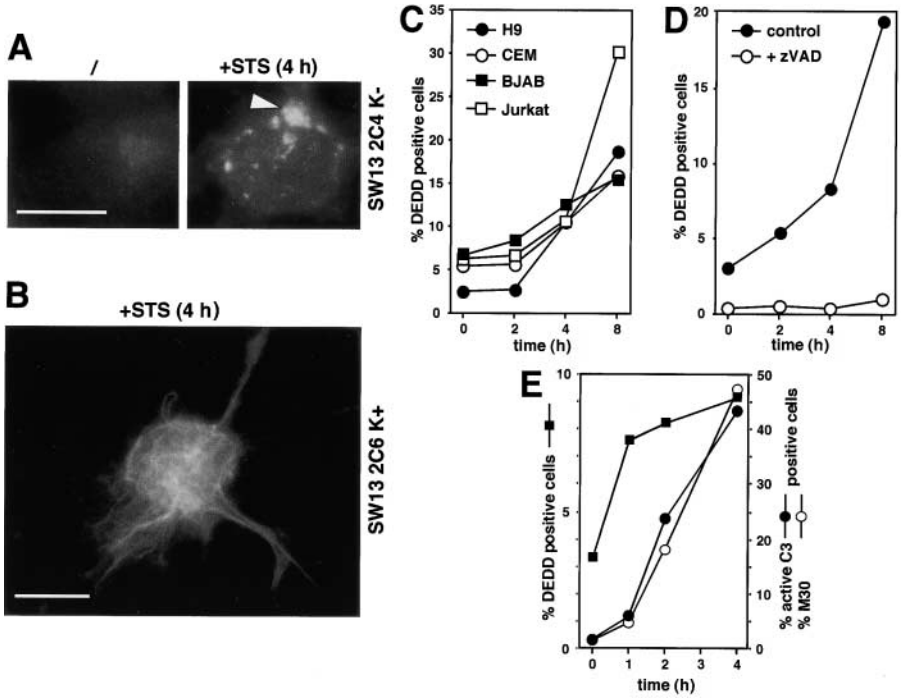

Figure 6. **Apoptosis-induced DEDD structures and aggregation are independent of keratins and occur before caspase-3 cleavage of K18.** (A) Non-apoptosing and apoptosing (STS 1 μM, 4 h) SW13 2C4 K− cells stained with DED3 and visualized in immunofluorescence. The arrowhead denotes one of the brightly staining DEDD structures only found in apoptosing cells. (B) SW13 cells reconstituted with K8/K18 (2C6 K+) also reconstituted apoptotic DEDD filaments following STS treatment (1 μM, 4 h). Bar, 10 μm. (C) Lymphoid cell lines treated with STS for 0, 2, 4, and 8 h and stained for intracellular DEDD using DED3 and FACS analysis. (D) HeLa cells treated with STS (1 μM) for 0, 2, 4, and 8 h in the absence or presence of pretreatment with zVAD-fmk (50 μM, 30 min) and analyzed as in C. (E) HeLa cells treated with STS (1 μM) for 0, 1, 2, 3, and 4 h and stained with DED3, M30, or anti-active caspase-3.

cells (Fig. 5 C). At later stages of apoptosis, both caspase-3–cleaved K18 and DEDD colocalized in the cytoplasmic inclusions (Fig. 5 D). Again, we detected some inclusions that stained positive for cleaved K18 but negative for DEDD (Fig. 5 C, arrowhead). Using EM, we confirmed that DEDD colocalizes with cleaved K18 in these structures (Fig. 5 E) and, in the final stage of apoptosis, these inclusions migrated into cytoplasmic blebs (Fig. 5 D; unpublished data).

DEDD aggregation precedes activation of caspase-3 and cleavage of K18

To determine the sequence of events involving DEDD changes and K18 cleavage, and to determine whether the ability of DEDD to stain IF like structures required the presence of cytokeratins, we compared the keratin deficient cell line SW13 with SW13 cells stably expressing K8 and K18 (Fig. 6). In the SW13 cells that do not express keratins, induction of apoptosis by STS resulted in detection of DEDD in intracellular aggregates (Fig. 6 A, arrowhead). This result indicated that the aggregation of DEDD is independent of its association with cytokeratins. However, in the K8/K18-expressing SW13 cells, DEDD stained in filaments that again colocalized largely with K18 (Fig. 6 B; unpublished data). To test whether the change of DEDD was generally occurring in cells lacking IF proteins, we treated a number of lymphoid cells with STS and stained for intracellular DEDD in a FACS-based analysis (Fig. 6 C). In all cases, DEDD staining increased during the course of apoptosis. The increase in intracellular DEDD staining could be prevented by pretreating cells with the poly-caspase inhibitor zVAD-fmk as shown for HeLa cells (Fig. 6 D), again confirming that active caspases were required for the increased staining of DEDD. Taken together, all data indicated the change of DEDD is independent of cytokeratins, suggesting that it precedes changes in the IF system during apoptosis, and that it may regulate these changes. To test whether DEDD played a regulatory role in the caspase-mediated cleavage of K18, we compared the kinetics of the DEDD apoptotic staining with activation of caspase-3 and cleavage of K18 by caspase-3 in HeLa cells (Fig. 6 E). After 1 h of STS treatment we detected few M30-positive cells by intracellular staining, whereas the DED3 staining had already reached ~70% of its maximal response. In this particular experiment, after 4 h of treatment, almost all cells positive for DEDD also contained caspase-3–cleaved K18. Comparison of these events with the appearance of processed caspase-3 revealed that the kinetics of caspase-3 activation in these cells were indistinguishable from the kinetics of K18 cleavage, confirming that M30 staining was effective in quantifying the activation of caspase-3. These data were also confirmed by quantifying immunofluorescence data (unpublished data). The observation that the increase in staining and aggregation of DEDD are both independent of keratins and precedes activation of caspase-3 and K18 cleavage by caspase-3 suggests that DEDD may function in facilitating caspase-3 cleavage of K18.

DEDD and active caspase-3 localize to intermediate filaments during apoptosis

Though the biochemical and immunofluorescence data suggested a role for DEDD in mediating caspase-3 cleavage of K18, DEDD filaments only partially overlapped with caspase-3–cleaved K18 (Fig. 5 C). If DEDD is involved in the recruitment and activation of caspase-3 one would expect that active caspase-3 would primarily be associated with DEDD and not with K18. To test this hypothesis we treated MCF7-C3 cells with STS and stained with M30 and an antibody specific for the neoepitope in caspase-3 that forms after processing of caspase-3 between its active subunits (Fig. 7 A). The result demonstrated that there was only a partial colocalization of active caspase-3 with caspase-3–cleaved

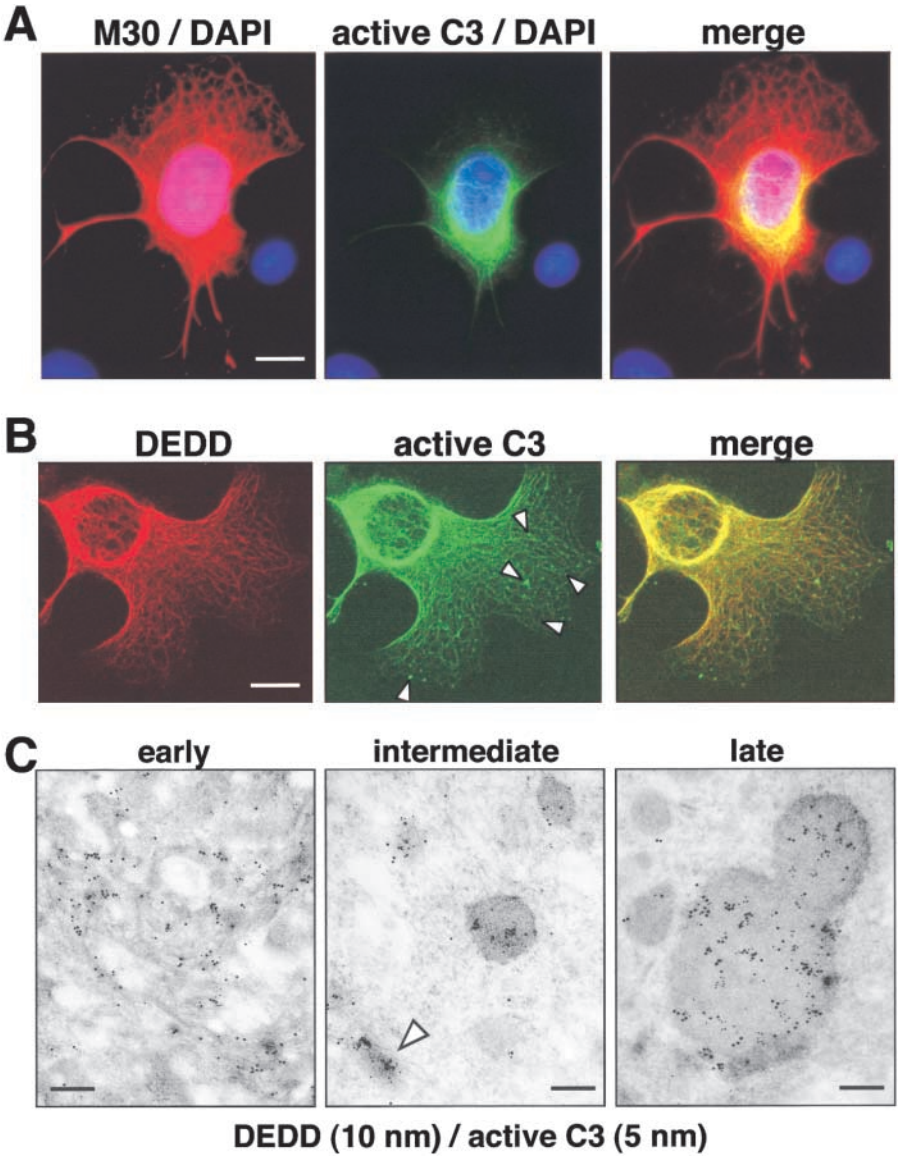

Figure 7. **DEDD colocalizes with active caspase-3 during apoptosis.** (A) Apoptotic MCF7-C3 cells (1 μM STS, 4 h) costained with anti-active caspase-3 and M30. Bar, 10 μm. (B) Apoptotic MCF7-C3 cells (1 μM STS, 4 h) costained with anti-active caspase-3–FITC and DED3. Bar, 10 μm. Arrowheads denote small granules that were only positive for active caspase-3. (C) HeLa cells treated with TRAIL (1 μg/ml, 2 h) were subjected to immunoelectron microscopy. DEDD (10-nm gold particles) and active, caspase-3 (5-nm gold particles) were found to colocalize in filaments (early stages of apoptosis), small intracytoplasmic inclusions (intermediate stages of apoptosis), and in large coalesced intracytoplasmic inclusions (late stages of apoptosis). The arrowhead denotes a residual DEDD and active caspase-3–positive filament. Bar, 250 nm.

K18 in the perinuclear area of the cells, a spatial relationship reminiscent of DEDD and M30. We then directly costained MCF7-C3 cells treated with STS for DEDD and active caspase-3 (Fig. 7 B). In all cells, of which only one is shown, all filamentous DEDD stained positive for active caspase-3, suggesting that DEDD recruited caspase-3 to IFs. Upon closer inspection of these stainings we detected small granular structures containing active caspase-3 which did not stain for DEDD and that seemed to emanate from the filamentous structures (Fig. 7 B, arrowheads).

Filaments formed by DEDD in apoptosing cells were somewhat reminiscent of filaments that were shown to form upon overexpression of certain DED proteins. It had been shown that these "death effector filaments" colocalized with and activated caspase-8 (Siegel et al., 1998). Therefore, we stained STS-treated MCF7-C3 cells for DEDD and caspase-8 (unpublished data) but found no colocalization of DEDD filaments with caspase-8, suggesting that DEDD specifically colocalized with processed caspase-3.

To determine the association of processed caspase-3 and DEDD during different stages of apoptosis, we performed an EM analysis of HeLa cells treated with TRAIL. In early stages of apoptosis, DEDD colocalized with active caspase-3 on IFs (Fig. 7 C, left). At intermediate stages when IF filaments started to disintegrate, DEDD colocalized with active caspase-3 on the remaining sheaves of IF structures (Fig. 7 C, middle, arrowhead) and in small inclusions. At later stages, these small inclusions fused to larger structures still containing DEDD and active caspase-3 (Fig. 7 C, right). This analysis was supported by a kinetic analysis of STS-treated MCF7-C3 cells using immunofluorescence microscopy (unpublished data) and demonstrated that the colocalization of caspase-3 subunits with DEDD is not restricted to a cell line that stably expresses exogenous procaspase-3 but can also be found between endogenous DEDD and endogenous active caspase-3. These data strongly suggested a direct interaction between DEDD and caspase-3 that results in activation of caspase-3.

Caspase-3 is recruited to K8/K18 during apoptosis

Though procaspase-3 is evenly distributed in the cytosol in most cells, active caspase-3 localizes with certain keratins to intracellular inclusions in late stage apoptosing epithelial

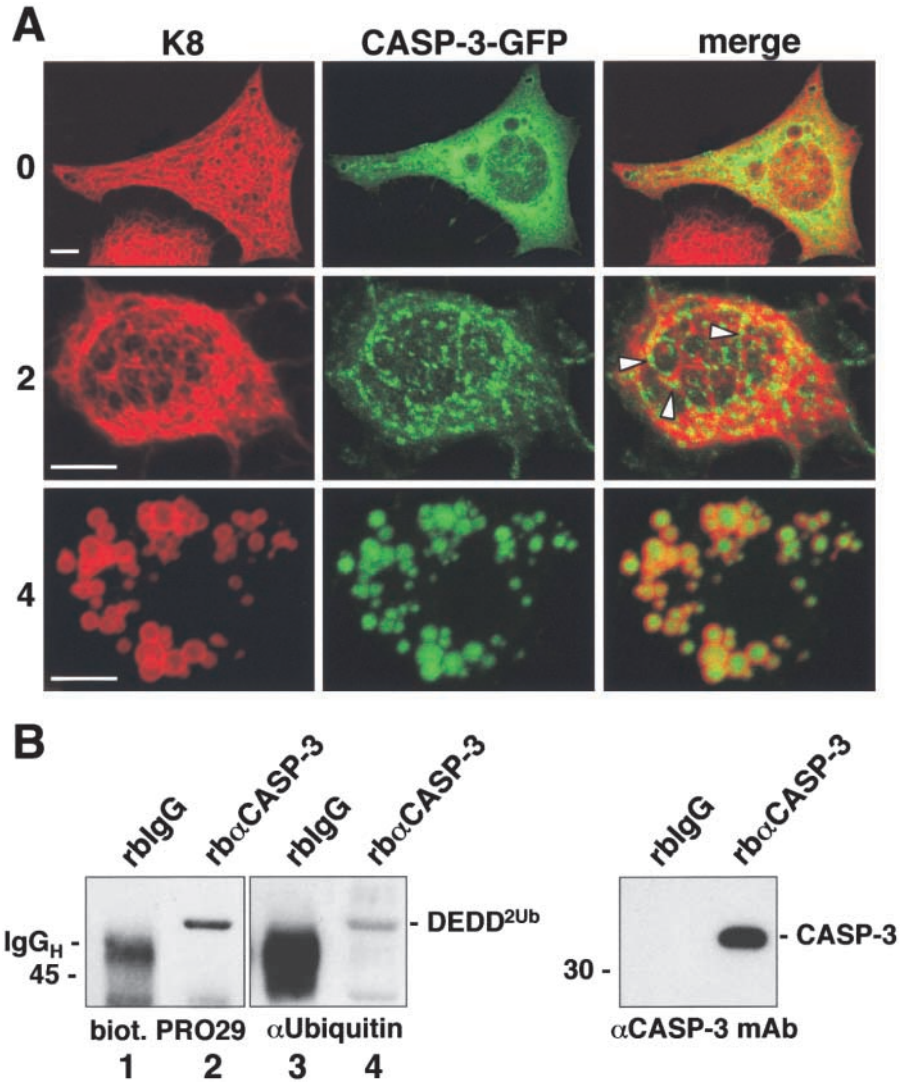

Figure 8. **Caspase-3 is recruited to IFs and associates with DEDD.** (A) MCF7 cells were transiently transfected with procaspase-3–GFP, treated with STS (0, 2 and 4 h) and stained for K8. Cells were analyzed by confocal microscopy. Shown are two-dimensional pictures of three-dimensional images, which were created using 20 overlaying 0.5 μm z-sections. Merge, overlay of GFP fluorescence and K8 staining. Arrowheads denote caspase-3–GFP positivity on IFs. A three-dimensional image of this panel is depicted in Video 1 (available online at http://www.jcb.org/cgi/content/full/jcb.200112124/DC1). Bar, 10 μm. (B) Immunoprecipitation of caspase-3 from MCF7-C3 (with a rabbit polyclonal caspase-3 antibody) coimmunoprecipitated DEDD^{2Ub} as detected by biotinylated PRO29 and anti-ubiquitin mAb (left two panels). Control blot (right) with a different caspase-3 (CASP-3) mAb detected efficient caspase-3 immunoprecipitation. Note, the same blot was probed sequentially in the order PRO29, anti-CASP-3, anti-ubiquitin. All M_r notations on left side of blots in kD.

cells (Caulin et al., 1997; MacFarlane et al., 2000). If keratin-bound DEDD is involved in the caspase-3 cleavage of keratins caspase-3 should be detectable at IFs. Due to the lack of anti–caspase-3 antibodies for adequate procaspase-3 detection in immunofluorescence microscopy, we transiently transfected MCF7 cells with a pro–caspase-3–GFP fusion protein and induced apoptosis by treating cells with STS. After fixation with paraformaldehyde cells were stained with anti-K8 (Fig. 8 A). In untreated cells caspase-3–GFP was detected throughout the cytosol with no significant colocalization with K8 and expression of the fusion protein did not affect the integrity of the IF system (Fig. 8 A, top row). Late after induction of apoptosis at 4 h of STS treatment both caspase-3–GFP and K8 were found in the same intracellular inclusions (Fig. 8 A, bottom row) in agreement with previous reports. However, at an earlier stage of apoptosis (2 h after STS treatment), caspase-3–GFP was found in small structures lining IF filaments mostly in the center of the cells (Fig. 8 A, middle row). The association of caspase-3 with K8 in early apoptosing cells was most evident in a three-dimensional movie (Video 1, available at http://www.jcb.org/cgi/content/full/jcb.200112124/DC1). To directly test whether DEDD associates with procaspase-3 prior to induction of apoptosis we immunoprecipitated procaspase-3 from MCF7-C3 cell lysates and immunoblotted with biotinylated PRO29 (Fig. 8 B). The only DEDD-reactive band that specifically associated with caspase-3 was the 54-kD band of DEDD. Because our analysis of this band had identified it as diubiquitinated DEDD, we now reprobed that blot with an anti-ubiquitin mAb and confirmed that this protein is both reactive with anti-DEDD and anti-ubiquitin antibodies. Our data suggested that procaspase-3 in MCF7-C3 cells is associated with diubiquitinated DEDD, and that DEDD mediates recruitment of procaspase-3 to the IFs during apoptosis, leading to cleavage of IF proteins such as K18 or vimentin.

DEDD is involved in activation of caspase-3, cleavage of K18, and execution of apoptosis

To directly determine the role of DEDD in apoptosis of epithelial cells, we made use of the RNAi technology to downregulate selected mRNAs (Elbashir et al., 2001). HeLa cells were mock treated or treated with lamin A/C or DEDD-specific siRNAs and tested for expression of lamin A/C and DEDD proteins by Western blotting (Fig. 9 A). Treatment of cells with the lamin A/C siRNA resulted in a strong re-

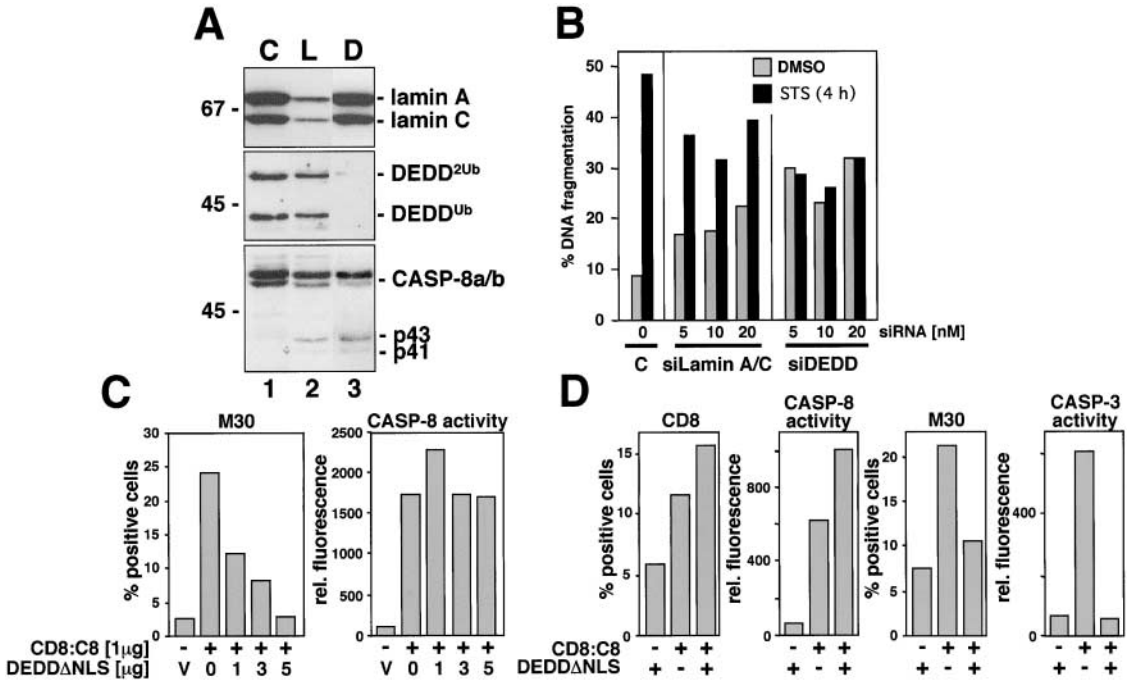

Figure 9. **DEDD is important in epithelial cells for activation of caspase-3.** (A) RNAi was performed in HeLa cells by transfection with lamin A/C or DEDD siRNA. Western blots were probed with anti-lamin A/C (top) and PRO29 (middle). Protein loading was determined by anti-caspase 8 (bottom). C, control (mock transfected); L, 10 nM lamin A/C siRNA; D, 10 nM DEDD siRNA. All M_r notations on left side of blots in kD. (B) DNA fragmentation was assessed in HeLa cells treated with 5, 10, and 20 nM lamin A/C or DEDD siRNA in comparison to control (transfection reagent only). As quantified by a Cy3-conjugated luciferase siRNA, uptake of siRNA at the above concentrations was >90% (not depicted). (C) Transient transfection of 293T cells with 1 μg of a CD8-caspase-8 fusion (CD8:C8) and increasing amounts of dominant negative DEDD (DEDDΔNLS). FACS analysis of M30 intracellular staining detected a decrease in fluorescence that correlated with increasing DEDDΔNLS dosage. Equal activation of caspase-8 was confirmed by a fluorogenic caspase assay with the IETD-AFC substrate. V, vector. (D) HeLa cells transfected with DEDDΔNLS, CD8:C8, or both indicated a reduction in caspase-3 activation as well as K18 cleavage in the presence of dominant negative DEDD. Cells were stained with anti-CD8 and M30 for FACS analysis. Caspase-8 and -3 activities were measured by a fluorogenic caspase assay with the IETD-AFC and DEVD-AFC substrates, respectively.

duction of lamin A/C expression but did not affect expression of $DEDD^{Ub}$ or $DEDD^{2Ub}$ (no unmodified DEDD was detected in this experiment). Conversely, treatment of cells with the DEDD siRNA did not alter expression of lamin A/C, but resulted in a profound loss of both DEDD proteins. Neither siRNA significantly decreased the amount of caspase-8 which we used as a loading control. However, we realized that both siRNAs were somewhat toxic for HeLa cells, as we also detected the caspase-8 cleavage intermediates p43 and p41 (Medema et al., 1997) indicating that transfection of cells with the siRNAs caused weak apoptosis which was not observed in the mock transfected cells (Fig. 9 A, lane 1). To test whether DEDD was important for execution of apoptosis in HeLa cells, DNA fragmentation was quantified in siRNA-transfected cells treated with STS for 4 h (Fig. 9 B). Three different concentrations of siRNA confirmed that lamin A/C siRNA treated-cells were sensitive to STS induced DNA fragmentation. However, at the same three concentrations of DEDD, siRNA cells were resistant to STS-induced DNA fragmentation but exhibited a higher level of basal DNA fragmentation without apoptotic stimulus when compared with cells transfected with lamin A/C or luciferase siRNAs (unpublished data). This could be due to dual functions of DEDD at its two intracellular locations, the nucleus and the cytoplasm. Downregulation of DEDD in nucleoli may reduce the cell viability before the effect of the downregulation of DEDD in the cytosol could be seen. Therefore, we sought a way to selectively modulate DEDD in the cytosol.

Overexpression of a cystolic DEDD mutant with a deletion of all three nuclear localization signals (DEDDΔNLS) does not induce apoptosis (Schickling et al. 2001). To test whether DEDDΔNLS would interfere with the function of endogenous DEDD in the cytosol, we utilized a fusion protein consisting of the extracellular and transmembrane domains of CD8 linked to the caspase-8 enzymatic domains (CD8:C8). This construct had been described to induce apoptosis upon overexpression by specific activation of caspase-8 through induced proximity facilitated by the constitutively dimerizing Ig domains of CD8 (Martin et al., 1998). Overexpression of CD8:C8 caused caspase-3 cleavage of K18 as detected by M30 staining of transfected cells quantified by flow cytometry (Fig. 9 C). However, cotransfection of increasing amounts of DEDDΔNLS with CD8:C8 inhibited cleavage of K18 at position D397 to background levels. Coexpression of DEDDΔNLS did not affect the amount of active caspase-8 (Fig. 9 C, right) generated by CD8:C8 expression, suggesting that DEDDΔNLS acted by specifically inhibiting the degradation of K18 by caspase-3.

The dominant negative effect of DEDDΔNLS suggests that it could either bind to IF proteins, directly blocking access of caspase-3 to K18, or it could prevent activation of

caspase-3 in the cytosol. To test whether cleavage of K18 by caspase-3 was inhibited by DEDDΔNLS we transiently transfected HeLa cells with the CD8:C8 construct with DEDDΔNLS (Fig. 9 D). Expression of the CD8:C8 construct was monitored by staining for surface CD8 by flow cytometry. Again, coexpression of DEDDΔNLS did not affect expression of CD8:C8 or the amount of caspase-8 generated in these cells (Fig. 9 D). As in 293T cells, DEDDΔNLS inhibited cleavage of K18 by caspase-3 and prevented the appearance of caspase-3 like activity in the cytosol. These data strongly argue that DEDDΔNLS does not simply block K18 cleavage by binding to K18, thereby blocking access of caspase-3 to K18 but rather that DEDDΔNLS regulates activation or activity of caspase-3 in the cytosol. This argument is further supported by transient expression of DEDDΔNLS–GFP fusion proteins in MCF7-C3 cells which showed a diffuse cytosolic localization with no costaining with the IF system (unpublished data). Our experiments in Fig. 3 have demonstrated that DEDDΔNLS cannot be ubiquitinated. Therefore, the dominant negative effect of DEDDΔNLS may be due to its inability to move to the nucleus and/or its inability to be ubiquitinated, suggesting that ubiquitination may serve as an important functional regulator of DEDD. Taken together the data strongly point to DEDD as a regulator of the cleavage of K18 by caspase-3 and suggest that DEDD is involved in activation of caspase-3 which leads to DNA fragmentation in the tested cells.

Discussion

The apoptosis pathway is a chain of biochemical events that affects all parts of the cell resulting in its ordered disintegration. Today, ~120 dedicated apoptosis signaling proteins are known that facilitate and regulate this process. Many of these proteins carry specialized protein–protein interaction domains such as the DED that ensure the ordered activation of the main executioner in apoptosis, the caspases. Caspase-3 is the main effector caspase and consequently most of the known caspase substrates have been shown to be cleaved by caspase-3 most often at the expected DXXD cleavage site. Currently there are ~34,000 protein sequences in the NCBI data base which contain 40,000 putative DXXD motifs that could represent caspase-3 cleavage sites. However, only a relatively small number of ~100 caspase-3 substrates are known (Tan and Wang, 1998; Earnshaw et al., 1999). Caspases can be expressed in many intracellular compartments (Stegh and Peter, 2001) and all caspases have been shown to also be expressed in the biggest compartment, the cytosol. The question of how specificity of substrate cleavage is achieved in this compartment is only beginning to be elucidated. In other signaling pathways this is often achieved by utilizing scaffold proteins, adaptors that serve as platforms on which specific signaling complexes are formed. Examples for such proteins are SLP-76 for T cell receptor signaling (Pivniouk et al., 1998) or JIP for MAP kinase signaling (Yasuda et al., 1999). We postulate that DEDD represents such a protein in the apoptosis pathway. This conclusion is based on the following observations: (a) DEDD interacts with both procaspase-3 and its main substrate in epithelial cells, keratin 18; (b) upon overexpression DEDD localizes to nucleoli and colocalizes with active caspase-6 (Schickling et al., 2001); (c) active caspase-3 almost exclusively colocalizes with DEDD on IFs; (d) overexpression of a dominant negative mutant of DEDD inhibits activation of caspase-3; and (e) downregulation of DEDD using DEDD-specific siRNA inhibits STS-induced activation of caspase-3 (unpublished data) and DNA fragmentation.

DEDD2 has a similar structure to DEDD (Roth et al., 2002; Zhan et al., 2002; and this work). Like DEDD, DEDD2 localizes to nucleoli when overexpressed and acts proapoptotically from within the nucleus. Our experiments detecting endogenous proteins demonstrated that an antibody against the DED in DEDD2 showed the same remarkable staining as the DED3 antibody against the DED in DEDD. In both cases, the increase in staining and detection of brightly stained filamentous structures depended on activation of caspase-3. This strongly suggests that both proteins act together and may even respond to the same stimuli.

Due to its dual localization, DEDD may have different functions in the nucleus and the cytoplasm. We have shown that overexpression of DEDD in the nucleus affects DNA Pol I-dependent transcription of rDNA (Stegh et al., 1998; Schickling et al., 2001). Consistent with a nuclear function of DEDD, it was recently reported that DEDD (and DEDD2) interact with the TFIIIC102 subunit of the human transcription factor IIIC (Zhan et al., 2002). This finding together with our recent identification of endogenous DEDD as being in part a nucleolar protein (Schickling et al., 2001) suggests that DEDD plays a role in the general transcription machinery in the nucleus. This might explain why downregulation of total cellular DEDD in HeLa and MCF7 cells using DEDD-specific siRNA was more toxic to the cells than treatment with control siRNAs. However, the lack of induced DNA fragmentation after STS treatment suggests that DEDD is required for STS induced apoptosis. We conclude that this reflects DEDD's cytoplasmic function since overexpression of purely cytosolic DEDDΔNLS inhibited caspase-3 activation and cleavage of K18 in cells cotransfected with the caspase-8 activating killer construct CD8:caspase-8 (Martin et al., 1998). This activity of DEDDΔNLS could be due to two functional changes when compared to wild-type DEDD: the inability of the mutant protein to enter the nucleus or the lack of monoubiquitination. The most well-known function of ubiquitination is to target proteins for degradation by the proteasome. However, monoubiquitination has been shown to be involved in endocytosis of a number of cellular and viral proteins (for review see Hicke, 2001). The best-known monoubiquitinated proteins are histones (Busch and Goldknopf, 1981). Monoubiquitination of H2A and H2B has been shown to be involved in gene regulation (Spencer and Davie, 1999). However, only a fraction of histones are monoubiquitinated. In contrast, DEDD represents the most quantitatively monoubiquitinated protein known. Cleavage of diubiquitinated DEDD with cyanogen bromide revealed that two different fragments are modified (unpublished data), indicating that DEDD is monoubiquitinated at two different sites. Interestingly, it is diubiquitinated DEDD that coimmunoprecipitated with K18 or procaspase-3. We are currently testing whether monoubiquitination of DEDD is required for

these interactions to occur. Interestingly, no ubiquitinated DEDD could be detected in nucleoli-enriched fractions (Schickling et al., 2001; unpublished data), whereas in the cytosol of the same cells DEDD was mainly ubiquitinated. Therefore, mono- and diubiquitination could also regulate DEDD's intracellular localization.

Disintegration of the IF network is a general feature of apoptosing cells and cleavage of IF proteins is important for progression of apoptosis. Recent data indicate that IF proteins play a dynamic role during apoptosis by actively regulating the apoptotic process both positively and negatively. Vimentin is cleaved by caspases during apoptosis (Prasad et al., 1998; Morishima, 1999), generating a proapoptotic NH_2-terminal fragment (Byun et al., 2001). Cytokeratins 8 (K8) and 18 (K18), IF proteins present in primary and transformed simple epithelia, seem to negatively regulate the apoptosis sensitivity of certain cells such that K8 or K18 deficient epithelial cells are 100 times more sensitive to TNF than wild-type cells (Caulin et al., 2000). The moderation of TNF-induced apoptosis by K18 may be due to competition between K18 and TNF-RI for TRADD, a key TNF-RI adaptor protein (Inada et al., 2001). Another study reported that the lack of cytokeratins strongly sensitized hepatocytes to CD95 mediated apoptosis by allowing CD95 to be transported more efficiently to the cell surface (Gilbert et al., 2001). Many of the IF proteins contain conserved cleavage sites for caspase-3 or -7 (at the COOH terminus and in the center of the proteins) and for caspase-6 (in the center) (Caulin et al., 1997; Ku et al., 1997). Once IF filaments have collapsed after cleavage by caspases, many of the IF proteins can be found in specific intracellular inclusions (Caulin et al., 1997; MacFarlane et al., 2000). These spheroidal inclusions contain K8, cleaved K18, cleaved K19 but not K13/15/16, vimentin, and β-actin or tubulin (Caulin et al., 1997; MacFarlane et al., 2000). Interestingly, not only cleaved cytokeratins but also most, if not all, of the cytosolic pool of active caspase-3 were found sequestered in these structures during TRAIL induced apoptosis in MCF7 cells (MacFarlane et al., 2000). We now show that these inclusions which occur during a number of other apoptotic stimuli that activate caspase-3 contain both DEDD and DEDD2.

Detection of filamentous structures of active caspase-3 on IF branches precedes the formation of these inclusions, which also precisely colocalize with activated DEDD and DEDD2. Because DEDD is constitutively associated with K18 in nonapoptosing cells, DEDD likely changes its conformation while bound to K18. This conclusion is further supported by the finding that in keratin-free SW13 cells DEDD can be found in intracellular aggregates and not in K8/18-like filamentous structures. Reconstitution of SW13 cells with both K8 and K18 resulted in detection of DEDD filaments. We could detect no DEDD structures bound to vimentin in a vimentin expressing variant of SW13 cells (unpublished data), suggesting that binding of DEDD to the IF system is predominantly mediated through cytokeratins.

DEDD was found to be associated with K18 and significantly colocalized with K18 during immunofluorescence microscopy. DEDD almost completely colocalized with active caspase-3. Unexpectedly, colocalization of DEDD with caspase-3–cleaved K18 was only partial. However, consistent with DEDD's localization, active caspase-3 also only partially colocalized with caspase-3–cleaved K18. This finding could be explained by the properties of the IF system which has been shown to be highly dynamic (Prahlad et al., 1998; Windoffer and Leube, 1999). We propose that keratins after the initial caspase cleavage move away from caspase-3/DEDD complexes, explaining the apparent dissociation of active caspase-3/DEDD with cleaved K18. At the end stage of apoptosis when most inclusions have fused to larger structures DEDD, cleaved K18 and active caspase-3 again colocalize in most of these inclusions.

Several models may explain the function of the DEDD containing inclusions. It has been suggested that these inclusions could be the final graveyard for active caspases such as caspase-3, -7, and -9 (unpublished data). In this model, they would represent structures used to inactivate and dispose of active caspases. However, why only simple epithelial cells and not numerous other cell types would use this mechanism to dispose of caspases remains to be elucidated. It is more likely that these structures serve a specific function. Late during etoposide- and UV-induced apoptosis, most of these structures were found in cytoplasmic blebs which seemed to develop into apoptotic bodies (Fig. 5 D; unpublished data). This effect was not seen in STS treated cells, as STS has been shown to inhibit blebbing (Mills et al., 1998).

Based on the new findings in this work, we have developed a model of DEDD's function (Fig. 10). DEDD resides in the cytoplasm in an inactive form bound to a population of K18. Upon induction of apoptosis, a small amount of caspase-3 is activated (step I), causing a conformational change in DEDD (step II). This may attract and activate more caspase-3 (step III), which then leads to cleavage of DEDD-associated cytokeratins (step IV). This step is clearly evident by the complete colocalization of active caspase-3, DEDD, and K18. After cleavage of K18, the IF network collapses and DEDD, active caspases, and cleaved cytokeratins are found in intracellular inclusions which may subsequently migrate into cytoplasmic blebs (step V). Our data indicate that activation of caspase-3 is both upstream and downstream of DEDD. Caspase-3 activity is required both for the conformational change of DEDD as well as the cleavage of DEDD-associated IF proteins. Therefore, DEDD would provide a unique way for one effector caspase to be activated in two steps in the same compartment. According to our model, DEDD could act as an intracellular timer to ensure degradation of substrates by caspase-3 in an ordered fashion. The regulation of these two steps requires further study.

We recently demonstrated that when it is overexpressed, DEDD activates and colocalizes with active caspase-6 in nucleoli (Schickling et al., 2001). We now report that endogenous DEDD colocalizes with active caspase-3 on IFs. Caspase-6 and -3 are the major caspases required for disintegration of IF proteins (nuclear lamins and cytokeratins, respectively) which has been demonstrated to be an essential step in the morphological changes seen during apoptosis (Rao et al., 1996; Caulin et al., 1997; Ku et al., 1997). Future experiments will determine the exact mechanism how DEDD and DEDD2 regulate theses processes.

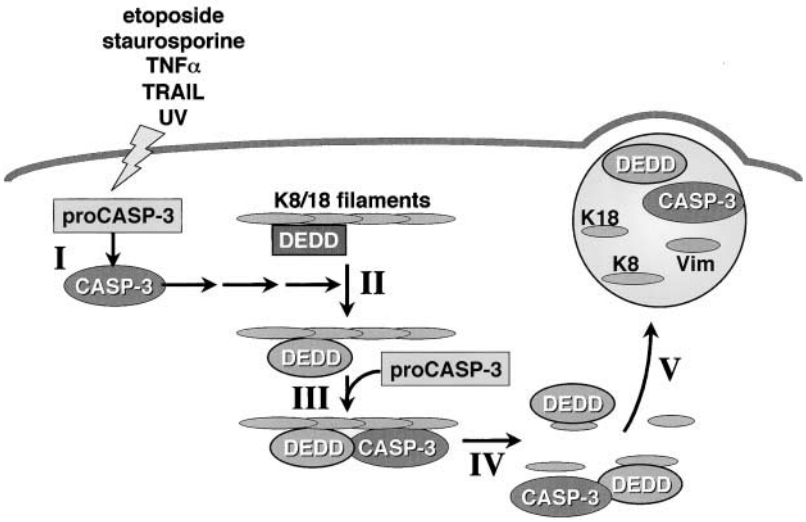

Figure 10. **Model of DEDD function during apoptosis.** In nonapoptosing cells, certain amounts of DEDD (likely in its diubiquitinated form) are constitutively associated with the K8/K18 network and/or procaspase-3. Upon induction of apoptosis by a variety of agents, early during apoptosis a small amount caspase-3 is activated (step I) likely involving mitochondria (not depicted). This population of caspase-3, via unknown mechanisms, aids directly or indirectly in the aggregation of DEDD. Apoptotic DEDD then concentrates caspase-3 at the K8/18 network leading to the activation of caspase-3. At this stage all three molecules are visualized as filamentous structures (step III). After disintegration of the filaments (step IV), intracytoplasmic proteinaceous inclusions are formed that also contain DEDD, DEDD2, active caspase-3, and IF proteins. These structures are later found in apoptotic cytoplasmic blebs (step V).

Materials and methods

Cell lines and reagents

HeLa, MCF7, Jurkat, H9, CEM, and BJAB cells were maintained in RPMI; SW13, A549, and 293T cells were maintained in DME in a humidified atmosphere (5% CO_2) at 37°C supplemented with L-glutamine, 100 μg/ml penicillin and streptomycin, and 10% heat-inactivated fetal calf serum (Sigma-Aldrich). ts20 and E36 cells were provided by X.J. Sun (University of Vermont, Burlington, VT) and maintained as previously described (Zhande et al., 2002). MCF7 stable transfectants (vector and caspase-3) (Janicke et al., 1998a) were supplemented with 100 μg/ml G418 and SW13 stable transfectants (vector and K8/K18) were supplemented with 400 μg/ml G418. The plasmids pcDNA3-3′FLAG-DEDD and pcDNA3-3′DEDD-FLAGΔNLS1-3 (for simplicity we refer to these constructs as DEDD-FLAG and DEDDΔNLS) have been described previously (Stegh et al., 1998; Schickling et al., 2001). pEGFP-N1-Caspase-3 (MacFarlane et al., 2000), pCEFL-CD8:C8 (Martin et al., 1998), and pMT123 (HA-Ubi) (Treier et al., 1994) were provided by M. MacFarlane (University of Leicester, Leicester, UK), M. Lenardo (National Institutes of Health, Bethesda, MD), and C. Pickart (Johns Hopkins University, Baltimore, MD), respectively.

Cloning of DEDD2 and generation of polyclonal anti-DEDD2 antiserum

TBLASTN searches of the human expressed sequence tag data base using the DEDD open reading frame identified a clone BE797255 from a small cell lung carcinoma library that contained a sequence that was highly homologous to 80% of the DEDD open reading frame. Sequencing of this clone which was obtained from the ATCC revealed an open reading frame coding for a protein of 326 amino acids that was 48% identical to DEDD (EMBL/GenBank/DDBJ accession no. for DEDD2 cloned in this work: AY125488). We then generated an antibody to the corresponding region within the DED (APGAAGGLARARSGLE) of DEDD2 which was used to generate the anti-DEDD antibody DED3. Although the DED between DEDD and DEDD2 are 47.5% identical the region of this 16–amino acid peptide only shared 2 identical amino acids. Subsequent tests revealed that the antibodies DED3 and anti-DEDD2 were specific for DEDD and DEDD2, respectively.

Induction of apoptosis

Apoptosis induction in cells used in immunofluorescence and intracellular FACS stainings was performed with the following conditions: 1 μM staurosporine (Sigma-Aldrich) for the indicated times, 1 μg/ml TRAIL (MacFarlane et al., 2000) for the indicated times, 200 μM etoposide (Sigma-Aldrich) for 24 h, 1 μg/ml cycloheximide plus 20 ng/ml TNFα for 12 h, or UV irradiated (100 kJ) and cultivated for 24 h after irradiation before harvesting. To block apoptosis, cells were pretreated for 30 min with 50 μM zVAD-fmk.

Western blot

Western blotting was performed as previously described (Schickling et al., 2001) with the following antibodies: PRO29 (previously called anti-DEDD1; Schickling et al., 2001) (1 μg/ml), biotinylated PRO29 (1 μg/ml), DED3 (previously called anti-DEDD2; Schickling et al., 2001) (1 μg/ml), anti-K8 (1 μg/ml; Sigma-Aldrich), anti-FADD (1 μg/ml; Transduction Laboratories), anti-FLAG (1 μg/ml; Sigma-Aldrich), anti-HA (1 μg/ml; Covance), anti-K18 (0.4 μg/ml; Santa Cruz Biotechnology, Inc.), anti-lamin A/C (0.4 μg/ml; Santa Cruz Biotechnology, Inc.), and anti-active caspase-3 (1:1,000; Cell Signaling Technologies). Goat anti–rabbit-Ig-HRP (1:15,000; Santa Cruz Biotechnology, Inc.) or isotype specific goat anti–mouse IgG-HRP (1:15,000; Southern Biotechnology) were used as secondary antibodies.

Immunofluorescence microscopy

Cells were grown on poly-prep slides (Sigma-Aldrich) and fixed with 2% paraformaldehyde for 20 min at room temperature. After the fixation the slides were washed three times with 50 mM NH_4Cl (in PBS) for 3 min, permeabilized in ice-cold PBS with 0.3% Triton X-100 (Sigma-Aldrich) for 1 min, washed with PBS-Mg (PBS + 1 mM $MgCl_2$), and incubated for 10 min in blocking solution (PBS, 0.01% saponin, 0.25% BSA and 0.02% NaN_3). The slides were incubated for 2 h at room temperature or overnight at 4°C with the indicated antibodies: DED3 (8 μg/ml), anti-K8 (5 μg/ml; Sigma-Aldrich), M30 (1:50; Roche), anti-active caspase-3–FITC (9 μg/ml; Pharmingen), and anti-DEDD2 (10 μg/ml). Peptide competition for the DED3 antibody was performed as previously described (Schickling et al., 2001). After washing with PBS-Mg, slides were incubated with secondary antibodies (5 μg/ml; Southern Biotechnology) and DAPI (2 μg/ml) for 1 h at room temperature, washed, and dehydrated in 100% ethanol. Coverslips were mounted onto the slides with Vectashield mounting medium (Vector Laboratories) and analyzed with an Axiovert S100 immunofluorescence microscope equipped with an Axiocam digital camera and software (Zeiss). Confocal pictures were taken and analyzed with a confocal microscope LSM 510 (Zeiss).

Intracellular FACS analysis

Cells were fixed for 30 min in methanol (−20°C), pelleted for 5 min at 500 *g*, and blocked for 30 min at room temperature in incubation buffer (PBS, 0.1% Tween 20, and 1% BSA). Primary antibodies were diluted in incubation buffer (DED3 10 μg/ml, M30 1:50, anti-CD8 10 μg/ml [Pharmingen], anti-active caspase-3–FITC 1:10) and incubated with the cells for 1 h at room temperature. Subsequently, the cells were washed with washing buffer (PBS, 0.1% Tween 20) and incubated with FITC-conjugated secondary antibodies (10 μg/ml; Southern Biotechnology) for 30 min at room temperature. The cells were washed twice and analyzed by fluorescence-activated cell sorter (FACScan; Becton Dickinson).

Electron microscopy and immunogold cytochemistry

Cells were fixed with a mixture of 4% formaldehyde and 0.1% glutaraldehyde in Dulbecco's PBS, pH 7.4, for 1 h at room temperature, spun down in a swing-out rotor at 3,000 *g*, rinsed in PBS, dehydrated in ethanol, and infiltrated with Unicryl resin from British Biocell International Ltd. The resin was polymerized with UV radiation (360 nm), at 4°C, according to the manufacturer's instructions. Ultrathin sections were blocked with normal goat serum, diluted 1:50 in PBS containing 1% BSA and 1% Tween 20, for 4 h at room temperature. Serial sections were incubated, for 18 h at 4°C, with antibodies to DEDD (DED3), β-actin, tubulin, vimentin, cytoker-

atins 8 and 18, and to the caspase-3 cleavage fragment of cytokeratin 18 (M30). These primary antibodies were all diluted (1 + 5) in PBS containing 1% normal goat serum, 1% BSA and 1% Tween 20 (PBSGAT). In control incubations, the primary antibodies were replaced with mouse IgG1 or normal rabbit serum (Dako Ltd.). Thorough washing in PBSGAT was followed by incubation, for 18 h at 4°C, in the appropriate goat-derived anti–mouse or –rabbit IgG (British Biocell International Ltd.). Secondary antibodies, adsorbed against human serum proteins and conjugated with 10 nm colloidal gold, were diluted 1:50 in PBSGAT. Sections incubated with mixtures of mouse- and rabbit-derived antibodies were subsequently labeled with a mixture of anti–mouse antibody conjugated with 10 nm gold and anti–rabbit antibody conjugated with 5 nm gold, respectively. Ultrathin sections were examined unstained or after staining with lead citrate and/or uranyl acetate.

Ubiquitination of DEDD

293T cells were transiently cotransfected by the calcium-precipitation method as previously described (Stegh et al., 1998) with DEDD-FLAG or DEDDΔNLS-FLAG in the presence of vector or pMT123 at the indicated amounts. Cells were harvested 24 h after transfection, lysed in sample buffer, and Western blots were probed with anti-FLAG. For IP, cells were lysed with 2% empigen (as described in Lowthert et al., 1995). Lysates were spun down and incubated with 10 μg anti-FADD 1C4 or anti-FLAG M2 (Sigma-Aldrich) and 50 μl of anti–mouse IgG1 beads (Sigma-Aldrich) at 4°C for 1 h rotating end to end. Beads were washed, resuspended in sample buffer, and Western blots were probed with anti-FLAG and HA.11 (Covance). 293T cells transiently transfected with vector or pMT123 were cultured for 4 h and treated with DMSO or 20 μM MG132 (Calbiochem) for 12 h. Cells were harvested, lysed in sample buffer, and Western blots were probed with PRO29. E36 and ts20 cells were maintained at the permissive temperature (30°C) or shifted to the restrictive temperature (40°C) for 12 h. Cells were harvested, lysed in sample buffer, and Western blots were probed with PRO29.

Characterization of DEDD in murine tissue

A piece of tissue (size dependent on organ) from C3H or Nit ± C57BL/6Jx129 mice (one female and one male each) was diced finely with a scalpel and put in 200–500 μl of lysis buffer (30 mM Tris, pH 7.5; 10% glycerol; 150 mM NaCl; 1% NP-40) plus inhibitors and incubated on ice for 30 min to 1 h before a brief sonication. Lysates were spun at 13,000 rpm for 7 min and the supernatant transferred to a new tube. 60 μg of protein were loaded per lane for Western blotting with PRO29.

Subcellular fractionation

Cells were harvested and lysed in ice-cold total lysis buffer composed of 250 mM NaCl; 50 mM HEPES, pH 7.0; 5 mM EDTA; 1% NP-40, *Complete*® protease inhibitors (Roche Molecular Biochemicals) for 60 min and sonicated (30 s, 20% intensity). Insoluble material was pelleted with 20,000 *g* for 15 min at 4°C. Supernatant (S) and pellet (P) were separated and resuspended in reducing sample buffer containing 5 M urea.

Immunoprecipitation of keratin 18 and caspase-3

HeLa cells were treated with 400 μM of etoposide, harvested, and lysed with 2% empigen lysis buffer as described previously (Lowthert et al., 1995). Lysates were spun (14,000 rpm, 15 min) and protein amount was quantified (Bio-Rad Laboratories). 3 mg of protein were incubated with 18 μg of anti-K18 (Santa Cruz Biotechnology, Inc.) or anti-FADD 1C4 at 4°C 1 h rotating end to end. Subsequently, 50 μl of resuspended anti–mouse IgG1-agarose beads (Sigma-Aldrich) were added to the lysate/antibody tubes and incubated overnight at 4°C rotating end to end. Following incubation, beads were washed four times with lysis buffer and resuspended in sample buffer. MCF7-C3 cells were lysed in 1% NP-40 lysis buffer (250 mM NaCl; 50 mM Hepes, pH 7.0; 5 mM EDTA; 1% Nonidet P-40, *Complete*®) for 1 h on ice. Lysates were (14,000 rpm, 15 min) and protein amount was quantified (Bio-Rad Laboratories). 3 mg of protein were incubated with 10 μg of anti–caspase-3 (Cell Signaling Technologies) or normal rabbit Ig (Santa Cruz Biotechnology, Inc.) at 4°C 1 h rotating end to end. Subsequently, 35 μl of resuspended protein A-Sepharose beads (Sigma-Aldrich) were added to the lysate/antibody tubes and incubated overnight at 4°C rotating end to end. After incubation, beads were washed four times with lysis buffer and resuspended in sample buffer.

RNAi and cytotoxicity assay

RNAi experiments were performed as previously described (Elbashir et al., 2001). Briefly, HeLa cells were transfected with DEDD, lamin A/C, or Cy3-luciferase siRNAs (Dharmacon) at the indicated amounts with Transit-TKO (Mirus) in 24-well plates according to manufacturer's instructions and incubated for 48 h. Cells were harvested and lysed in sample buffer for Western blotting or quantified for DNA fragmentation as previously described (Stegh et al., 1998).

Influence of DEDDDNLS on keratin 18 cleavage

293T or HeLa cells were transfected with the indicated amount of plasmid DNA either using the calcium-phosphate (293T) or *Superfect*™ (HeLa) following the manufacturer's protocol (QIAGEN). 24 h after transfection the cells were harvested and either intracellularly stained for cleaved keratin with M30 or lysed for quantification of caspase-3 and -8 activities with fluorogenic caspase substrates as previously described (Stegh et al., 2000).

Online supplemental material

Video 1 is available online at http://www.jcb.org/cgi/content/full/jcb.200112124/DC1. The three-dimensional image represented as a QuickTime video is taken from Fig. 8 (second row, right), and shows GFP-positive structures (green) aligning on intermediate filament strands (red) stained with anti-K8 after treating HeLa cells transfected with caspase-3–GFP with staurosporine for 2 h.

We are grateful to A. Murmann for help with the confocal analyses, Dr. M. Lenardo for providing the CD8:caspase-8 fusion construct, and Dr. A. Porter for providing the caspase-3 reconstituted MCF7 cells, respectively. We thank Drs. M. MacFarlane, C. Pickart, and X. Sun for providing the pEGFP-N1-caspase-3, HA-ubiquitin constructs, and the ts20 cells, respectively. We also thank Drs. T. Commisso and K. Hubner for performing the Western blot of mouse tissues.

J.C. Lee was supported by the Medical Scientist Training Grant from the National Institutes of Health. A.H. Stegh was supported by a stipend from the Boehringer Ingelheim Fonds.

Submitted: 24 December 2001
Revised: 18 July 2002
Accepted: 31 July 2002

References

Byun, Y., F. Chen, R. Chang, M. Trivedi, K.J. Green, and V.L. Cryns. 2001. Caspase cleavage of vimentin disrupts intermediate filaments and promotes apoptosis. *Cell Death Differ.* 8:443–450.

Busch, H., and I.L Goldknopf. 1981. Ubiquitin protein conjugates. *Mol. Cell Biochem.* 40:173–187.

Caulin, C., G.S. Salvesen, and R.G. Oshima. 1997. Caspase cleavage of keratin 18 and reorganization of intermediate filaments during epithelial cell apoptosis. *J. Cell Biol.* 138:1379–1394.

Caulin, C., C.F. Ware, T.M. Magin, and R.G. Oshima. 2000. Keratin-dependent, epithelial resistance to tumor necrosis factor-induced apoptosis. *J. Cell Biol.* 149:17–22.

Earnshaw, W.C. 1995. Nuclear changes in apoptosis. *Curr. Opin. Cell Biol.* 7:337–343.

Earnshaw, W.C., L.M. Martins, and S.H. Kaufmann. 1999. Mammalian caspases: structure, activation, substrates, and functions during apoptosis. *Annu. Rev. Biochem.* 68:383–424.

Elbashir, S.M., J. Harborth, W. Lendeckel, A. Yalcin, K. Weber, and T. Tuschl. 2001. Duplexes of 21-nucleotide RNAs mediate RNA interference in cultured mammalian cells. *Nature.* 411:494–498.

Gilbert, S., A. Loranger, N. Daigle, and N. Marceau. 2001. Simple epithelium keratins 8 and 18 provide resistance to Fas-mediated apoptosis. The protection occurs through a receptor-targeting modulation. *J. Cell Biol.* 154:763–773.

Hicke, L. 2001. Protein regulation by monoubiquitin. *Nat. Rev. Mol. Cell Biol.* 2:195–201.

Inada, H., I. Izawa, M. Nishizawa, E. Fujita, T. Kiyono, T. Takahashi, T. Momoi, and M. Inagaki. 2001. Keratin attenuates tumor necrosis factor-induced cytotoxicity through association with TRADD. *J. Cell Biol.* 155:415–426.

Janicke, R.U., P. Ng, M.L. Sprengart, and A.G. Porter. 1998a. Caspase-3 is required for alpha-fodrin cleavage but dispensable for cleavage of other death substrates in apoptosis. *J. Biol. Chem.* 273:15540–15545.

Janicke, R.U., M.L. Sprengart, M.R. Wati, and A.G. Porter. 1998b. Caspase-3 is required for DNA fragmentation and morphological changes associated with apoptosis. *J. Biol. Chem.* 273:9357–9360.

Ku, N.O., J. Liao, and M.B. Omary. 1997. Apoptosis generates stable fragments of human type I keratins. *J. Biol. Chem.* 272:33197–33203.

Ku, N.O., S. Azhar, and M.B. Omary. 2002. Keratin 8 phosphorylation by p38 ki-

nase regulates cellular keratin filament reorganization: modulation by a keratin 1-like disease causing mutation. *J. Biol. Chem.* 277:10775–10782.

Leers, M.P., W. Kolgen, V. Bjorklund, T. Bergman, G. Tribbick, B. Persson, P. Bjorklund, F.C. Ramaekers, B. Bjorklund, M. Nap, et al. 1999. Immunocytochemical detection and mapping of a cytokeratin 18 neo-epitope exposed during early apoptosis. *J. Pathol.* 187:567–572.

Lowthert, L.A., N.O. Ku, J. Liao, P.A. Coulombe, and M.B. Omary. 1995. Empigen BB: a useful detergent for solubilization and biochemical analysis of keratins. *Biochem. Biophys. Res. Commun.* 206:370–379.

MacFarlane, M., W. Merrison, D. Dinsdale, and G.M. Cohen. 2000. Active caspases and cleaved cytokeratins are sequestered into cytoplasmic inclusions in TRAIL-induced apoptosis. *J. Cell Biol.* 148:1239–1254.

Martin, D.A., R.M. Siegel, L. Zheng, and M.J. Lenardo. 1998. Membrane oligomerization and cleavage activates the caspase-8 (FLICE/MACHalpha1) death signal. *J. Biol. Chem.* 273:4345–4349.

Medema, J.P., C. Scaffidi, F.C. Kischkel, A. Shevchenko, M. Mann, P.H. Krammer, and M.E. Peter. 1997. FLICE is activated by association with the CD95 death-inducing signaling complex (DISC). *EMBO J.* 16:2794–2804.

Mills, J.C., N.L. Stone, J. Erhardt, and R.N. Pittman. 1998. Apoptotic membrane blebbing is regulated by myosin light chain phosphorylation. *J. Cell Biol.* 140:627–636.

Mimnaugh, E.G., H.Y. Chen, J.R. Davie, J.E. Celis, and L. Neckers. 1997. Rapid deubiquitination of nucleosomal histones in human tumor cells caused by proteasome inhibitors and stress response inducers: effects on replication, transcription, translation, and the cellular stress response. *Biochemistry.* 36: 14418–14429.

Morishima, N. 1999. Changes in nuclear morphology during apoptosis correlate with vimentin cleavage by different caspases located either upstream or downstream of Bcl-2 action. *Genes Cells.* 4:401–414.

Oshima, R.G. 2002. Apoptosis and keratin intermediate filaments. *Cell Death Differ.* 9:486–492.

Peter, M.E., A. Heufelder, and M.O. Hengartner. 1997. Advances in apoptosis research. *Proc. Natl. Acad. Sci. USA.* 94:12736–12737.

Pivniouk, V., E. Tsitsikov, P. Swinton, G. Rathbun, F.W. Alt, and R.S. Geha. 1998. Impaired viability and profound block in thymocyte development in mice lacking the adaptor protein SLP-76. *Cell.* 94:229–238.

Prahlad, V., M. Yoon, R.D. Moir, R.D. Vale, and R.D. Goldman. 1998. Rapid movements of vimentin on microtubule tracks: kinesin-dependent assembly of intermediate filament networks. *J. Cell Biol.* 143:159–170.

Prasad, S.C., P.J. Thraves, M.R. Kuettel, G.Y, Srinivasarao, A. Dritschilo, and V.A. Soldatenkov. 1998. Apoptosis-associated proteolysis of vimentin in human prostate epithelial tumor cells. *Biochem Biophys Res Commun.* 249:332–338.

Rao, L., D. Perez, and E. White. 1996. Lamin proteolysis facilitates nuclear events during apoptosis. *J. Cell Biol.* 135:1441–1455.

Roth, W., F. Stenner-Liewen, K. Pawlowski, A. Godzik, and J.C. Reed. 2002. Identification and characterization of DEDD2, a death effector domain-containing protein. *J. Biol. Chem.* 277:7501–7508.

Schickling, O., A.H. Stegh, J. Byrd, and M.E. Peter. 2001. Nuclear localization of DEDD leads to caspase-6 activation through its death effector domain and inhibition of RNA polymerase I dependent transcription. *Cell Death Differ.* 8:1157–1168.

Schubert, U., D.E. Ott, E.N. Chertova, R. Welker, U. Tessmer, M.F. Princiotta, J.R. Bennink, H.G. Krausslich, and J.W. Yewdell. 2000. Proteasome inhibition interferes with gag polyprotein processing, release, and maturation of HIV-1 and HIV-2. *Proc. Natl. Acad. Sci. USA.* 97:13057–13062.

Siegel, R.M., D.A. Martin, L. Zheng, S.Y. Ng, J. Bertin, J. Cohen, and M.J. Lenardo. 1998. Death-effector filaments: novel cytoplasmic structures that recruit caspases and trigger apoptosis. *J. Cell Biol.* 141:1243–1253.

Spencer, V.A., and J.R. Davie. 1999. Role of covalent modifications of histones in regulating gene expression. *Gene.* 240:1–12.

Stegh, A.H., H. Herrmann, S. Lampel, D. Weisenberger, K. Andrä, M. Seper, G. Wiche, P.H. Krammer, and M.E. Peter. 2000. Identification of the cytolinker plectin as a major early *in vivo* substrate for caspase-8 during CD95 and TNF-receptor mediated apoptosis. *Mol. Cell. Biol.* 20:5665–5679.

Stegh, A.H., and M.E. Peter. 2001. Apoptosis and caspases. *Cardiol. Clin.* 19:13–29.

Stegh, A.H., O. Schickling, A. Ehret, C. Scaffidi, C. Peterhänsel, G. Längst, T. Hoffmann, I. Grummt, P.H. Krammer, and M.E. Peter. 1998. DEDD, a novel death effector domain-containing protein, targeted to the nucleolus. *EMBO J.* 17:5974–5986.

Tan, X., and J.Y. Wang. 1998. The caspase-RB connection in cell death. *Trends Cell Biol.* 8:116–120.

Treier, M., L.M. Staszewski, and D. Bohmann. 1994. Ubiquitin-dependent c-Jun degradation in vivo is mediated by the delta domain. *Cell.* 78:787–798.

Windoffer, R., and R.E. Leube. 1999. Detection of cytokeratin dynamics by time-lapse fluorescence microscopy in living cells. *J. Cell Sci.* 112:4521–4534.

Wyllie, A.H., J.F. Kerr, and A.R. Currie. 1980. Cell death: the significance of apoptosis. *Int. Rev. Cytol.* 68:251–306.

Yasuda, J., A.J. Whitmarsh, J. Cavanagh, M. Sharma, and R.J. Davis. 1999. The JIP group of mitogen-activated protein kinase scaffold proteins. *Mol. Cell. Biol.* 19:7245–7254.

Zhan, Y., R. Hegde, S.M. Srinivasula, T. Fernandes-Alnemri, and E.S. Alnemri. 2002. Death effector domain-containing proteins DEDD and FLAME-3 form nuclear complexes with the TFIIIC102 subunit of human transcription factor IIIC. *Cell Death Differ.* 9:439–447.

Zhande, R., J.J. Mitchell, J. Wu, and X.J. Sun. 2002. Molecular mechanism of insulin-induced degradation of insulin receptor substrate 1. *Mol. Cell. Biol.* 22: 1016–1026.

Zheng, L., O. Schickling, M.E. Peter, and M. Lenardo. 2001. The death effector domain associated factor plays distinct regulatory roles in the nucleus and the cytoplasm. *J. Biol. Chem.* 276:31945–31952.